

1                   **NUMERICAL ANALYSIS OF THE MIXED FINITE ELEMENT**  
2                   **METHOD FOR THE NEUTRON DIFFUSION EIGENPROBLEM**  
3                   **WITH HETEROGENEOUS COEFFICIENTS**

4                   P. CIARLET JR.<sup>1</sup>, L. GIRET<sup>1,2</sup>, E. JAMELOT<sup>3,\*</sup> AND F.D. KPADONOU<sup>1,4</sup>

5                   **Abstract.** We study first the convergence of the finite element approximation of the mixed diffusion  
6 equations with a source term, in the case where the solution is of low regularity. Such a situation  
7 commonly arises in the presence of three or more intersecting material components with different  
8 characteristics. Then we focus on the approximation of the associated eigenvalue problem. We prove  
9 spectral correctness for this problem in the mixed setting. These studies are carried out without, and  
10 then with a domain decomposition method. The domain decomposition method can be non-matching  
11 in the sense that the traces of the finite element spaces may not fit at the interface between subdomains.  
12 Finally, numerical experiments illustrate the accuracy of the method.

13                   **Mathematics Subject Classification.** 65N25, 65N30, 82D75

14                   Received July 7, 2017. Accepted January 25, 2018.

15                   1. INTRODUCTION

16                   The multigroup neutron diffusion equation, which is an approximation of the multigroup neutron transport  
17 equation, is important in nuclear industry since it allows to model many nuclear reactor cores [16]. In the  
18 steady state case, it corresponds to a generalized eigenvalue problem. We propose here the numerical analysis  
19 of this problem in the case of a discretization with mixed finite elements, possibly with a domain decomposition  
20 method. We focus on the one group of energy case which is the base block of the multigroup case. This paper is  
21 thus the extension of [13], where the authors proposed the numerical analysis of the one-group neutron diffusion  
22 equation with a source term, discretized with mixed finite elements, with matching and non-matching domain  
23 decomposition methods.

24                   Nuclear reactor cores often have a Cartesian geometry. In Figure 1a, we draw a top view of a PWR-like  
25 core model. Each square, which represents a part of the reflector or an assembly, is made itself of cells, which  
26 are rectangular cuboids of  $\mathbb{R}^3$ . In Figure 1b, we make a zoom on a patch of six ( $3 \times 2$ ) assemblies: each

---

*Keywords and phrases:* Diffusion equation, low-regularity solution, mixed formulation, eigenproblem, domain decomposition methods.

<sup>1</sup> POEMS, ENSTA ParisTech, CNRS, INRIA, 828 Bd des Maréchaux, 91762 Palaiseau Cedex, France.

<sup>2</sup> DEN-Service d'Etudes des Réacteurs et de Mathématiques Appliquées-SERMA, LLPR, CEA, Université Paris-Saclay, 91191 Gif-sur-Yvette Cedex, France.

<sup>3</sup> DEN-Service de Thermo-hydraulique et de Mécanique des Fluides-STMF, LMSF, CEA, Université Paris-Saclay, 91191 Gif-sur-Yvette Cedex, France.

<sup>4</sup> Laboratoire de Mathématiques de Versailles, UVSQ, 45 Av des Etats-Unis, 78035 Versailles Cedex, France.

\* Corresponding author: [erell.jamelot@cea.fr](mailto:erell.jamelot@cea.fr)

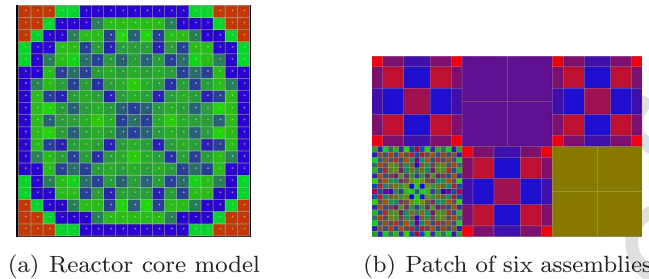


FIGURE 1. 2D depiction of a PWR core and a zoom on six assemblies.

colored square represents a cell containing fuel, absorbing or reflector material. In our model, the coefficients are polynomial (possibly constant) in each cell [16, 23, 24]. The global domain of the reactor core (see again Fig. 1a) is represented by a rectangular cuboid of  $\mathbb{R}^3$ . In practice the coefficients characterizing the materials may differ from one cell to another by a factor of order 10 or more.

The outline is as follows. In Section 2, we introduce the notations, and recall basic mathematical definitions. In the next section, we provide the main abstract tool that enables us to characterize the so-called low-regularity solutions, that is piecewise  $H^{1+r}$  solutions with an exponent  $r > 0$  that can be (arbitrarily) small. Then in Section 4, we solve the diffusion equation written in mixed form, with either a source term, or as an eigenproblem. We recall that the approximation of eigenvalue problems has been studied among others by Osborn et al. in [1, 27], and in particular by Boffi et al. [4, 5, 6] when the eigenproblem is in a mixed form. In our case however, their theory does not ensure the spectral correctness of the approximation so we design a new proof to obtain this result. On the other hand, we can adapt the work of Boffi et al. [8] to exhibit a convergence rate for the eigenvalues. For the discretization, we choose the well-known Raviart-Thomas-Nédélec finite element. Then in Sections 5 and 6, we consider the same problems, solved now with the help of a Domain Decomposition method: the DD+ $L^2$ -jumps method. Finally, we analyze the numerical capabilities of the DD+ $L^2$ -jumps method, before giving some concluding remarks.

## 2. GEOMETRY, HILBERT SPACES AND NOTATIONS

Throughout the paper,  $C$  is used to denote a generic positive constant which is independent of the meshsize, the triangulation and the quantities/fields of interest. We also use the shorthand notation  $A \lesssim B$  for the inequality  $A \leq CB$ , where  $A$  and  $B$  are two scalar quantities, and  $C$  is a generic constant. Respectively,  $A \approx B$  for the inequalities  $A \lesssim B$  and  $B \lesssim A$ .

Vector-valued (resp. tensor-valued) function spaces are written in boldface character (resp. blackboard characters); for the latter, the index *sym* indicates symmetric fields. Given an open set  $O \in \mathbb{R}^d$ ,  $d = 1, 2, 3$ , we use the notation  $(\cdot|\cdot)_{0,O}$  (respectively  $\|\cdot\|_{0,O}$ ) for the  $L^2(O)$  and  $\mathbf{L}^2(O) := (L^2(O))^d$  scalar products (resp. norms). More generally,  $(\cdot|\cdot)_{s,O}$  and  $\|\cdot\|_{s,O}$  (respectively  $|\cdot|_{s,O}$ ) denote the scalar product and norm (resp. semi-norm) of the Sobolev spaces  $H^s(O)$  and  $\mathbf{H}^s(O) := (H^s(O))^d$  for  $s \in \mathbb{R}$  (resp. for  $s > 0$ ).

If moreover the boundary  $\partial O$  is Lipschitz,  $\mathbf{n}$  denotes the unit outward normal vector field to  $\partial O$ . Finally, it is assumed that the reader is familiar with vector-valued function spaces related to the diffusion equation, such as  $\mathbf{H}(\text{div}; O)$ ,  $\mathbf{H}_0(\text{div}; O)$ , etc.

We let  $\mathcal{R}$  be a bounded, connected and open subset of  $\mathbb{R}^d$ , having a Lipschitz boundary which is piecewise smooth. We split  $\mathcal{R}$  into  $N$  open disjoint parts  $\{\mathcal{R}_i\}_{1 \leq i \leq N}$  with Lipschitz, piecewise smooth boundaries:  $\overline{\mathcal{R}} = \cup_{1 \leq i \leq N} \overline{\mathcal{R}_i}$  and the set  $\{\mathcal{R}_i\}_{1 \leq i \leq N}$  is called a partition of  $\mathcal{R}$ . For a field  $v$  defined over  $\mathcal{R}$ , we shall use the notations  $v_i = v|_{\mathcal{R}_i}$ , for  $1 \leq i \leq N$ .

60 Given a partition  $\{\mathcal{R}_i\}_{1 \leq i \leq N}$  of  $\mathcal{R}$ , we introduce function spaces with piecewise regular elements:

$$\begin{aligned} \mathcal{P}H^s(\mathcal{R}) &= \{ \psi \in L^2(\mathcal{R}) \mid \psi_i \in H^s(\mathcal{R}_i), 1 \leq i \leq N \}, \quad s > 0; \\ \mathcal{P}W^{1,\infty}(\mathcal{R}) &= \{ D \in L^\infty(\mathcal{R}) \mid D_i \in W^{1,\infty}(\mathcal{R}_i), 1 \leq i \leq N \}. \end{aligned}$$

61 We recall that for a piecewise smooth  $\psi \in \mathcal{P}H^s(\mathcal{R})$ ,  $\|\psi\|_{\mathcal{P}H^s(\mathcal{R})}^2 = \sum_{i=1}^N \|\psi\|_{s,\mathcal{R}_i}^2$ . Similarly for elements of  
62  $\mathcal{P}W^{1,\infty}(\mathcal{R})$ .

### 63 3. SETTING OF THE MODEL

64 Given a source term  $S_f \in L^2(\mathcal{R})$ , we consider the following neutron diffusion equation, with vanishing  
65 Dirichlet boundary condition. In its primal form, it is written:

66 Find  $\phi \in H_0^1(\mathcal{R})$  such that:

$$- \operatorname{div} D \mathbf{grad} \phi + \Sigma_a \phi = S_f \text{ in } \mathcal{R} \quad (3.1)$$

67 where  $\phi$ ,  $D$ , and  $\Sigma_a$  denote respectively the neutron flux, the diffusion coefficient and the macroscopic absorption  
68 cross section. Finally,  $S_f$  denotes the fission source. When  $S_f$  depends on  $\phi$ , the steady state neutron diffusion  
69 equation is a generalized eigenvalue problem. It reads (one group of energy):

70 Find  $\phi \in H_0^1(\mathcal{R}) \setminus \{0\}$ ,  $\lambda \in \mathbb{R}$  such that:

$$- \operatorname{div} D \mathbf{grad} \phi + \Sigma_a \phi = \lambda \nu \Sigma_f \phi \text{ in } \mathcal{R} \quad (3.2)$$

71 where  $\nu \Sigma_f$  is the fission yield times the macroscopic fission cross section. Under the assumption that the  
72 coefficients  $D$ ,  $\Sigma_a$  and  $\nu \Sigma_f$  are positive, the physical solution corresponds to the smallest  $\lambda \geq 0$  [12, 16]. When  
73 this problem is solved using the inverse power iteration, the source problem (3.1) corresponds to one iteration  
74 step, which further justifies its study.

75 When solving the neutron diffusion equation,  $D$  is scalar-valued. From now on and unless otherwise speci-  
76 fied, we adopt the more general setting of a (symmetric) tensor-valued coefficient  $D$ . The coefficients defining  
77 Problems (3.1) and (3.2) satisfy the assumptions:

$$\begin{cases} (D, \Sigma_a, \nu \Sigma_f) \in \mathbb{L}_{sym}^\infty(\mathcal{R}) \times L^\infty(\mathcal{R}) \times L^\infty(\mathcal{R}), \\ \exists D_*, D_* > 0, \forall \mathbf{z} \in \mathbb{R}^d, D_* \|\mathbf{z}\|^2 \leq (D\mathbf{z}, \mathbf{z}) \leq D_* \|\mathbf{z}\|^2 \text{ a.e. in } \mathcal{R}, \\ \exists (\Sigma_a)_*, (\Sigma_a)^* > 0, 0 < (\Sigma_a)_* \leq \Sigma_a \leq (\Sigma_a)^* \text{ a.e. in } \mathcal{R}, \\ 0 \leq \nu \Sigma_f \text{ a.e. in } \mathcal{R}, \nu \Sigma_f \neq 0. \end{cases} \quad (3.3)$$

78 In particular, it can happen that  $\nu \Sigma_f$  vanishes on some regions. Also, it is well known that Problem (3.1) is  
79 equivalent to the following variational formulation:

80 Find  $\phi \in H_0^1(\mathcal{R})$  such that  $\forall \psi \in H_0^1(\mathcal{R})$ :

$$\int_{\mathcal{R}} D \mathbf{grad} \phi \cdot \mathbf{grad} \psi + \int_{\mathcal{R}} \Sigma_a \phi \psi = \int_{\mathcal{R}} S_f \psi. \quad (3.4)$$

81 Under the assumptions (3.3) on the coefficients, the primal problem (3.1) is well-posed, in the sense that  
82 for all  $S_f \in L^2(\mathcal{R})$ , there exists one and only one  $\phi \in H_0^1(\mathcal{R})$  that solves (3.1), and in addition there holds  
83  $\|\phi\|_{1,\mathcal{R}} \lesssim \|S_f\|_{0,\mathcal{R}}$ . We recall that under additional mild assumptions on the coefficients, the solution  $\phi$  has  
84 some extra regularity (see [9, 14] and [13], Prop. 1).

**Proposition 3.1.** *Let  $D \in \mathcal{PW}_{sym}^{1,\infty}(\mathcal{R})$  and  $\Sigma_\alpha \in \mathcal{PW}^{1,\infty}(\mathcal{R})$  satisfy (3.3). There exists  $r_{\max} \in ]0, 1]$ , called the regularity exponent, such that for all source terms  $S_f \in L^2(\mathcal{R})$ , the solution  $\phi \in H^1(\mathcal{R})$  to Problem (3.1) belongs to  $\bigcap_{0 \leq r < r_{\max}} \mathcal{P}H^{1+r}(\mathcal{R})$  ( $r_{\max} < 1$ ) or  $\mathcal{P}H^2(\mathcal{R})$  ( $r_{\max} = 1$ ) with continuous dependence:*

$$\forall r \in [0, r_{\max}[, \|\phi\|_{\mathcal{P}H^{1+r}(\mathcal{R})} \lesssim \|S_f\|_{0,\mathcal{R}} \quad (r_{\max} < 1) \quad \text{or} \quad \|\phi\|_{\mathcal{P}H^2(\mathcal{R})} \lesssim \|S_f\|_{0,\mathcal{R}} \quad (r_{\max} = 1).$$

In the following, we study the two different problems, the source problem (3.1) and the eigenvalue problem (3.2). Unless otherwise specified, we keep the assumptions of Proposition 3.1 throughout the paper. Since cross-points are allowed in our model, cf. Figure 1a, and in accordance with [9], the low-regularity case corresponds precisely to

$$r_{\max} < 1/2.$$

For the eigenvalue problem, the analysis is carried out for eigenfunctions which can be either low-regularity functions or “smooth” functions.

**Remark 3.2.** Instead of imposing a vanishing Dirichlet boundary condition in the model, one can consider a vanishing Neumann boundary condition  $D \mathbf{grad} \phi \cdot \mathbf{n} = 0$  on  $\partial\mathcal{R}$ . Under some slight restrictions on the geometry, one can also consider a vanishing Fourier boundary condition  $\mu_F \phi + D \mathbf{grad} \phi \cdot \mathbf{n} = 0$  on  $\partial\mathcal{R}$ , with  $\mu_F > 0$ . In the latter case, the restriction is that the coefficient  $D$  is smooth in a neighborhood of the boundary. The theory and numerical analysis written hereafter still apply.

## 4. THE PLAIN CASE

We start our study with the neutron diffusion problem without domain decomposition method: we call it the plain case. In this section, we use the function space:

$$\mathbf{X} = \{ \xi := (\mathbf{q}, \psi) \in \mathbf{H}(\text{div}, \mathcal{R}) \times L^2(\mathcal{R}) \}, \quad \|\xi\|_{\mathbf{X}} := \left( \|\mathbf{q}\|_{\mathbf{H}(\text{div}, \mathcal{R})}^2 + \|\psi\|_{0,\mathcal{R}}^2 \right)^{1/2}.$$

From now on, we use the notations:  $\zeta = (\mathbf{p}, \phi)$  and  $\xi = (\mathbf{q}, \psi)$ .

### 4.1. Setting of the mixed variational formulation

Starting from the solution  $\phi$  to (3.1), if one lets  $\mathbf{p} := -D \mathbf{grad} \phi \in \mathbf{L}^2(\mathcal{R})$ , known as the neutron current, one may write the neutron diffusion problem as:

Find  $(\mathbf{p}, \phi) \in \mathbf{H}(\text{div}, \mathcal{R}) \times H_0^1(\mathcal{R})$  such that:

$$\begin{cases} -D^{-1} \mathbf{p} - \mathbf{grad} \phi = 0 & \text{in } \mathcal{R}, \\ \text{div } \mathbf{p} + \Sigma_\alpha \phi = S_f & \text{in } \mathcal{R}. \end{cases} \quad (4.1)$$

Solving the mixed problem (4.1) is actually equivalent to solving (3.1), as the result below recalls.

**Theorem 4.1.** *Let  $D$  satisfy (3.3). The solution  $(\mathbf{p}, \phi) \in \mathbf{H}(\text{div}, \mathcal{R}) \times H_0^1(\mathcal{R})$  to (4.1) is such that  $\phi$  is a solution to (3.1) with the same data. Conversely, the solution  $\phi \in H_0^1(\mathcal{R})$  to (3.1) is such that  $(-D \mathbf{grad} \phi, \phi) \in \mathbf{H}(\text{div}, \mathcal{R}) \times H_0^1(\mathcal{R})$  is a solution to (4.1) with the same data.*

In practice, writing the diffusion equation in its mixed form allows to compute precisely both the solution and its gradient: it avoids the propagation of the numerical error from the solution to its gradient. In order to obtain the variational formulation for the mixed problem (4.1), we consider any test functions  $\mathbf{q} \in \mathbf{H}(\text{div}, \mathcal{R})$  and  $\psi \in L^2(\mathcal{R})$ , we multiply the first equation of (4.1) by  $\mathbf{q}$ , the second equation of (4.1) by  $\psi \in L^2(\mathcal{R})$ , and

116 we integrate over  $\mathcal{R}$ . We sum the contributions to reach:

$$\int_{\mathcal{R}} (-D^{-1} \mathbf{p} \cdot \mathbf{q} - \mathbf{grad} \phi \cdot \mathbf{q} + \psi \operatorname{div} \mathbf{p} + \Sigma_a \phi \psi) = \int_{\mathcal{R}} S_f \psi. \quad (4.2)$$

117 We recall that  $\phi \in H_0^1(\mathcal{R})$ . One can integrate by parts to remove the first order derivatives of  $\phi$ :

$$- \int_{\mathcal{R}} \mathbf{grad} \phi \cdot \mathbf{q} = \int_{\mathcal{R}} \phi \operatorname{div} \mathbf{q}.$$

118 Hence, the regularity requirement on the solution can be lowered to  $\phi \in L^2(\mathcal{R})$ , and we find that the solution  
119 to (4.1) also solves:

120 Find  $(\mathbf{p}, \phi) \in \mathbf{X}$ , such that  $\forall (\mathbf{q}, \psi) \in \mathbf{X}$ :

$$\int_{\mathcal{R}} (-D^{-1} \mathbf{p} \cdot \mathbf{q} + \phi \operatorname{div} \mathbf{q} + \psi \operatorname{div} \mathbf{p} + \Sigma_a \phi \psi) = \int_{\mathcal{R}} S_f \psi. \quad (4.3)$$

121 We define the bilinear forms:

$$a : \begin{cases} \mathbf{H}(\operatorname{div}, \mathcal{R}) \times \mathbf{H}(\operatorname{div}, \mathcal{R}) \rightarrow \mathbb{R} \\ (\mathbf{p}, \mathbf{q}) \mapsto \int_{\mathcal{R}} -D^{-1} \mathbf{p} \cdot \mathbf{q} \end{cases} ; \quad (4.4)$$

122

$$b : \begin{cases} \mathbf{H}(\operatorname{div}, \mathcal{R}) \times L^2(\mathcal{R}) \rightarrow \mathbb{R} \\ (\mathbf{q}, \psi) \mapsto \int_{\mathcal{R}} \psi \operatorname{div} \mathbf{q} \end{cases} ; \quad (4.5)$$

123

$$t : \begin{cases} L^2(\mathcal{R}) \times L^2(\mathcal{R}) \rightarrow \mathbb{R} \\ (\phi, \psi) \mapsto \int_{\mathcal{R}} \Sigma_a \phi \psi \end{cases} ; \quad (4.6)$$

124 and:

$$c : \begin{cases} \mathbf{X} \times \mathbf{X} \rightarrow \mathbb{R} \\ (\zeta, \xi) \mapsto a(\mathbf{p}, \mathbf{q}) + b(\mathbf{q}, \phi) + b(\mathbf{p}, \psi) + t(\phi, \psi) \end{cases} . \quad (4.7)$$

125 **Remark 4.2.** The form  $c(\cdot, \cdot)$  is symmetric as soon as the tensor field  $D$  is symmetric.

126 We consider the linear form:

$$f : \begin{cases} \mathbf{X} \rightarrow \mathbb{R} \\ \xi \mapsto \int_{\mathcal{R}} S_f \psi \end{cases} . \quad (4.8)$$

127 We may rewrite the variational formulation (4.3) as:

128 Find  $\zeta \in \mathbf{X}$  such that  $\forall \xi \in \mathbf{X}$ :

$$c(\zeta, \xi) = f(\xi). \quad (4.9)$$

129 **Theorem 4.3.** *The solution  $\zeta = (\mathbf{p}, \phi)$  to (4.9) satisfies (4.1). Hence, problems (4.9) and (4.1) are equivalent.*

## 130 4.2. Well-posedness of the mixed formulation

131 We now recall how to obtain the well-posedness of (4.9) by proving in particular an inf-sup condition.

132 **Theorem 4.4.** *Let  $D$  and  $\Sigma_a$  satisfy (3.3). Then, there exists a unique solution  $\zeta \in \mathbf{X}$  to the mixed variational*  
 133 *formulation (4.9).*

134 *Proof.* Since the form  $c(\cdot, \cdot)$  is symmetric, the inf-sup condition yields the claim. This condition writes:

$$\exists \eta > 0, \quad \inf_{\zeta \in \mathbf{X}} \sup_{\xi \in \mathbf{X}} \frac{c(\zeta, \xi)}{\|\zeta\|_{\mathbf{X}} \|\xi\|_{\mathbf{X}}} \geq \eta. \quad (4.10)$$

135 To achieve (4.10), a possible choice is:

$$\begin{cases} \mathbf{q} = -\mathbf{p} \in \mathbf{H}(\operatorname{div}, \mathcal{R}), \\ \psi = \frac{1}{2}\phi + \frac{1}{2}(\Sigma_a)^{-1} \operatorname{div} \mathbf{p} \in L^2(\mathcal{R}). \end{cases} \quad (4.11)$$

136 It holds  $\|\zeta\|_{\mathbf{X}} \geq v \|\xi\|_{\mathbf{X}}$ , with  $v := (1 + \frac{1}{4}((\Sigma_a)_*)^{-2})^{-1/2}$ . The bound on  $c$  reads:

$$c(\zeta, \xi) \geq \gamma v \|\zeta\|_{\mathbf{X}} \|\xi\|_{\mathbf{X}},$$

137 with  $\gamma := \min((D^*)^{-1}, \frac{1}{2}(\Sigma_a)_*, \frac{1}{2}((\Sigma_a)^*)^{-1})$ . □

## 138 4.3. Discretization

139 We study conforming discretizations of the variational formulation (4.9). To fix ideas, we use a family of  
 140 triangulations, indexed by a parameter  $h$ , which is classically chosen as the largest diameter of elements of the  
 141 triangulation. We introduce discrete, finite-dimensional, spaces indexed by  $h$  as follows:

$$\mathbf{Q}_h \subset \mathbf{H}(\operatorname{div}, \mathcal{R}), \quad \text{and } L_h \subset L^2(\mathcal{R}).$$

142 For approximation purposes, and following Definition 2.14 in [17], we assume that  $(\mathbf{Q}_h)_h$ , resp.  $(L_h)_h$  have the  
 143 *approximability property* in the sense that

$$\begin{aligned} \forall \mathbf{q} \in \mathbf{H}(\operatorname{div}, \mathcal{R}), \quad \lim_{h \rightarrow 0} \left( \inf_{\mathbf{q}_h \in \mathbf{Q}_h} \|\mathbf{q} - \mathbf{q}_h\|_{\mathbf{H}(\operatorname{div}, \mathcal{R})} \right) &= 0, \\ \forall \psi \in L^2(\mathcal{R}), \quad \lim_{h \rightarrow 0} \left( \inf_{\psi_h \in L_h} \|\psi - \psi_h\|_{0, \mathcal{R}} \right) &= 0, \end{aligned} \quad (4.12)$$

144 and also that  $L_h$  includes the subspace  $L_h^0$  of piecewise constant fields on the triangulation.

145 We impose:  $\operatorname{div} \mathbf{Q}_h \subset L_h$ .

146 We endow  $\mathbf{Q}_h$  with the norm  $\|\cdot\|_{\mathbf{H}(\operatorname{div}, \mathcal{R})}$ , while  $L_h$  is endowed with  $\|\cdot\|_{0, \mathcal{R}}$ .

We finally define:

$$\mathbf{X}_h = \{ \xi_h := (\mathbf{q}_h, \psi_h) \in \mathbf{Q}_h \times L_h \}, \quad \text{endowed with } \|\cdot\|_{\mathbf{X}}.$$

147 The conforming discretization of the variational formulation (4.9) reads:

148 Find  $(\mathbf{p}_h, \phi_h) \in \mathbf{X}_h$ , such that  $\forall (\mathbf{q}_h, \psi_h) \in \mathbf{X}_h$ :

$$a(\mathbf{p}_h, \mathbf{q}_h) + b(\mathbf{q}_h, \phi_h) + b(\mathbf{p}_h, \psi_h) + t(\phi_h, \psi_h) = (S_f, \psi_h)_{0, \mathcal{R}}. \quad (4.13)$$

149 Or equivalently:

$$\text{Find } \zeta_h \in \mathbf{X}_h \text{ such that } \forall \xi_h \in \mathbf{X}_h, \quad c(\zeta_h, \xi_h) = f(\xi_h). \quad (4.14)$$

150 For later use, we denote  $\pi^0$  the  $L^2(\mathcal{R})$  orthogonal projector on its subspace  $L_h^0$ . By construction, it holds  
151  $\text{range}(\pi^0) = L_h^0$  where  $\pi^0$  is defined by:

$$\forall \psi \in L^2(\mathcal{R}), \forall \psi_h \in L_h^0, \quad (\pi^0 \psi - \psi, \psi_h)_{0, \mathcal{R}} = 0.$$

152 According to Proposition 1.135 of [17]:

$$\begin{aligned} \forall z \in L^2(\mathcal{R}), \quad \|z - \pi^0 z\|_{0, \mathcal{R}} &\lesssim \|z\|_{0, \mathcal{R}}, \\ \forall z \in \mathcal{P}H^1(\mathcal{R}), \quad \|z - \pi^0 z\|_{0, \mathcal{R}} &\lesssim h \|z\|_{\mathcal{P}H^1(\mathcal{R})}, \\ \forall z \in \mathcal{P}W^{1, \infty}(\mathcal{R}), \quad \|z - \pi^0 z\|_{\infty, \mathcal{R}} &\lesssim h \|z\|_{\mathcal{P}W^{1, \infty}(\mathcal{R})}. \end{aligned} \quad (4.15)$$

153 For the last two inequalities, the result holds provided that the triangulations are conforming with respect to  
154 the partition, namely for all triangulations, for all elements  $K$  of a triangulation, it holds that there exists  
155  $1 \leq i \leq N$  such that  $K \subset \overline{\mathcal{R}_i}$ . Similar results hold on subsets of  $\mathcal{R}$ .

#### 156 4.4. Discrete inf-sup condition

157 The discrete inf-sup condition to be found writes:

$$\exists \eta_h > 0, \quad \inf_{\zeta_h \in \mathbf{X}_h} \sup_{\xi_h \in \mathbf{X}_h} \frac{c(\zeta_h, \xi_h)}{\|\zeta_h\|_{\mathbf{X}} \|\xi_h\|_{\mathbf{X}}} \geq \eta_h. \quad (4.16)$$

158 Once (4.16) is achieved, one obtains existence and uniqueness of the discrete solution  $\zeta_h$ , hence the corresponding  
159 linear system is well-posed. More generally, our aim is to obtain that  $(\eta_h)_h$  is uniformly bounded away from 0.  
160 In this sense, one has at hand a *uniform discrete inf-sup condition* (udisc), from which the error analysis can  
161 classically be derived.

162 **Theorem 4.5.** *Let  $D$ , resp.  $\Sigma_a \in \mathcal{P}W^{1, \infty}(\mathcal{R})$ , satisfy (3.3). The discrete inf-sup condition (4.16) is fulfilled.*  
163 *Moreover, it is a uniform discrete inf-sup condition.*

164 *Proof.* In order to prove the discrete inf-sup condition, we use the same method as for the continuous inf-  
165 sup condition (cf. proof of Thm. 4.4). One can remark that if  $\Sigma_a$  is piecewise-constant,  $\frac{1}{2}(\Sigma_a)^{-1} \text{div } \mathbf{p}_h$  is  
166 automatically in  $L_h$ .

167 Otherwise, we project  $(\Sigma_a)^{-1}$  on the piecewise-constant functions. One modifies (4.11) by choosing:

$$\begin{cases} \mathbf{q}_h = -\mathbf{p}_h \in \mathbf{Q}_h, \\ \psi_h = \frac{1}{2}\phi_h + \frac{1}{2}\pi^0((\Sigma_a)^{-1}) \text{div } \mathbf{p}_h \in L_h. \end{cases}$$

168 Using (4.15) with  $z = (\Sigma_a)^{-1}$  yields  $\|(\Sigma_a)^{-1} - \pi^0((\Sigma_a)^{-1})\|_{\infty, \mathcal{R}} \lesssim h$ , which allows us to derive again a udisc in  
169 this more general case.  $\square$

#### 4.5. Numerical analysis of the source problem

We consider the neutron diffusion equation assuming that  $D$ , resp.  $\Sigma_a \in \mathcal{P}W^{1,\infty}(\mathcal{R})$ , satisfy (3.3). Under the assumptions of Section 4.3, it follows from the previous study that  $\lim_{h \rightarrow 0} \|\zeta - \zeta_h\|_{\mathbf{X}} = 0$ . We find below a sharper bound of the error  $\|\zeta - \zeta_h\|_{\mathbf{X}}$  by using Proposition 3.1. In order to obtain optimal *a priori* error estimates, we must know the regularity of the solution to problem (3.1). Since we have assumed that the source term  $S_f$  belongs to  $L^2(\mathcal{R})$ , we already know that  $\|\phi\|_{1,\mathcal{R}} \lesssim \|S_f\|_{0,\mathcal{R}}$ . Moreover, under the assumptions of Proposition 3.1, the solution  $\phi$  has some extra regularity, and the low-regularity case corresponds to  $r_{\max} < 1/2$  there. This is the case that we are focusing on now. In this setting, the field  $\mathbf{p} := -D \mathbf{grad} \phi$  automatically belongs to  $\mathcal{P}\mathbf{H}^r(\mathcal{R})$ , for  $0 \leq r < r_{\max}$ . We suppose in addition that

$$\exists \mu \in ]0, r_{\max}[, \quad S_f \in \mathcal{P}H^\mu(\mathcal{R}).$$

Then we have  $\mathbf{p} \in \mathcal{P}H^\mu(\mathcal{R})$  (recall  $\mathcal{P}H^\mu(\mathcal{R}) = H^\mu(\mathcal{R})$  for  $\mu < 1/2$ ). We will use this hypothesis on  $S_f$  to carry on the calculations of the error estimates.

We recall below the definition of the Raviart-Thomas-Nédélec (or RTN) finite element [26, 28]. Let  $(K_\ell)_{1 \leq \ell \leq L}$  be a conforming mesh, or triangulation, of  $\bar{\mathcal{R}}$  made of parallelepipeds (a mesh, or triangulation, is said to be conforming if in every  $K_\ell$ ,  $D$  and  $\Sigma_a$  are smooth). Let  $P(K_\ell)$  be the set of polynomials defined over  $K_\ell$ . For integer values  $l, m, p \geq 0$ , we consider the following subspace of  $P(K_\ell)$ :

$$Q_{l,m,p}(K_\ell) = \left\{ q(x, y, z) \in P(K_\ell) \mid q(x, y, z) = \sum_{e,j,k=0}^{l,m,p} a_{e,j,k} x^e y^j z^k, a_{e,j,k} \in \mathbb{R} \right\}.$$

For integer  $k \geq 0$ , let us set  $k' = k + 1$  and introduce the vector polynomial space:

$$\mathbf{D}_k(K_\ell) = [Q_{k',k,k}(K_\ell) \times \mathbf{0} \times \mathbf{0}] \oplus [\mathbf{0} \times Q_{k,k',k}(K_\ell) \times \mathbf{0}] \oplus [\mathbf{0} \times \mathbf{0} \times Q_{k,k,k'}(K_\ell)].$$

We can now define the RTN $_{[k]}$  finite element subspace of  $\mathbf{H}(\text{div}, \mathcal{R}) \times L^2(\mathcal{R})$ :

$$\begin{aligned} \mathbf{Q}_h^k &= \{ \mathbf{q} \in \mathbf{H}(\text{div}, \mathcal{R}) \mid \forall \ell \in \{1, \dots, L\}, \mathbf{q}|_{K_\ell} \in \mathbf{D}_k(K_\ell) \}, \\ L_h^k &= \{ \psi \in L^2(\mathcal{R}) \mid \forall \ell \in \{1, \dots, L\}, \psi|_{K_\ell} \in Q_{k,k,k}(K_\ell) \}. \end{aligned} \quad (4.17)$$

As required, it holds  $\text{div} \mathbf{Q}_h^k \subset L_h^k$  and  $L_h^0 \subset L_h^k$ . We recall that for any  $\mathbf{q}$  in  $\mathbf{H}(\text{div}, \mathcal{R})$ , its RTN $_{[k]}$ -interpolant  $\mathbf{q}_R^k \in \mathbf{Q}_h^k$  satisfies:

$$\forall \psi_h \in L_h^k, \quad b(\mathbf{q} - \mathbf{q}_R^k, \psi_h) = 0. \quad (4.18)$$

In addition thanks to the commuting diagram property, cf. Section 2.5.2 of [7], it holds

$$\forall \mathbf{q} \in \mathbf{H}(\text{div}, \mathcal{R}), \quad \text{div} \mathbf{q}_R^0 = \pi^0(\text{div} \mathbf{q}). \quad (4.19)$$

Let  $\mathbf{q} \in \mathbf{H}^r(\mathcal{R})$ , such that  $\text{div} \mathbf{q} \in H^s(\mathcal{R})$ ,  $0 < r, s < r_{\max}$ . According to Lemma 3.3 of [3]:

$$\begin{aligned} \|\mathbf{q} - \mathbf{q}_R^0\|_{0,\mathcal{R}} &\lesssim (h^r |\mathbf{q}|_{r,\mathcal{R}} + h \|\text{div} \mathbf{q}\|_{0,\mathcal{R}}), \\ \|\text{div}(\mathbf{q} - \mathbf{q}_R^0)\|_{0,\mathcal{R}} &\lesssim h^s |\text{div} \mathbf{q}|_{s,\mathcal{R}}. \end{aligned} \quad (4.20)$$

Similar results hold on subsets of  $\mathcal{R}$ , provided the discretizations are conforming.



192 **Remark 4.6.** If one chooses another discretization, all results presented hereafter hold provided the estimates  
 193 (4.20) remain true. For instance, for the RTN<sub>[k]</sub> finite element defined on tetrahedral triangulations of  $\overline{\mathcal{R}}$ , cf.  
 194 Section 2.3.1 of [7]. To prove (4.20) in this case, one has simply to apply the results of Section 3.2 from [3].  
 195 On the other hand, provided that the field  $\mathbf{q}$  and its divergence are “smooth” in the sense that they belong to  
 196  $\mathcal{P}H^{m+1}(\mathcal{R})$  for some integer  $m \geq 0$ , using the RTN<sub>[m]</sub> finite element one can recover interpolation estimates in  
 197  $O(h^{m+1})$ , cf. Section 2.5.5 in [7]. For meshes made of affine elements such as tetrahedra or parallelepipeds, the  
 198 approximation estimate (4.20-top) does not require the term with the divergence (see, e.g. [7], Sect. 2.5.1).

#### 199 4.5.1. A priori error estimates

200 Since we focus on the low-regularity case, we choose the RTN<sub>[0]</sub> finite element, i.e.  $\mathbf{X}_h = \mathbf{Q}_h^0 \times L_h^0$ . If the  
 201 solution is “smooth”, one can increase the order of the RTN finite element. This will be used in particular in  
 202 Section 4.6.2 for the study of the error on the eigenvalues. According to first Strang’s Lemma [17] and because  
 203  $(1 + \|c\|(\eta_h)^{-1}) \lesssim 1$ , the error reads:

$$\|\zeta - \zeta_h\|_{\mathbf{X}} \lesssim \inf_{\xi_h \in \mathbf{X}_h} \|\zeta - \xi_h\|_{\mathbf{X}}. \quad (4.21)$$

204 **Theorem 4.7.** *Under the assumptions of Proposition 3.1, it holds, with  $r_{\max} < 1/2$ :*

$$\begin{aligned} & \forall \mu \in ]0, r_{\max}[ , \forall S_f \in H^\mu(\mathcal{R}), \\ & \|\mathbf{p} - \mathbf{p}_h\|_{\mathbf{H}(\text{div}, \mathcal{R})} + \|\phi - \phi_h\|_{0, \mathcal{R}} \lesssim h^\mu \|S_f\|_{\mu, \mathcal{R}}. \end{aligned} \quad (4.22)$$

205 **Remark 4.8.** In particular, for “smooth data”  $S_f$ , i.e.  $S_f \in H^{r_{\max}}(\mathcal{R})$ , one expects a convergence rate at  
 206 least in  $h^{r_{\max} - \eta}$  for  $\eta > 0$  arbitrary small: by a slight *abuse of notation* there and in the sequel, we shall write  
 207  $h^{r_{\max}}$ . Also, the previous analysis can be extended to the case where  $r_{\max}$  is in  $[1/2, 1]$  and  $\mu < r_{\max}$  (or  $\mu \leq 1$   
 208 if  $r_{\max} = 1$ ). Furthermore, for a “smooth” solution, one may recover a convergence rate like  $O(h^{m+1})$  for an  
 209 RTN<sub>[m]</sub> discretization of order  $m \geq 0$ .

210 *Proof.* Choosing  $\xi_h = (\mathbf{p}_R^0, \pi^0 \phi) \in \mathbf{X}_h$ , then thanks to the *a priori* estimates (4.15) and (4.20), it follows that:

$$\begin{aligned} \|\zeta - \xi_h\|_{\mathbf{X}}^2 &= \|\mathbf{p} - \mathbf{p}_R^0\|_{\mathbf{H}(\text{div}, \mathcal{R})}^2 + \|\phi - \pi^0 \phi\|_{0, \mathcal{R}}^2 \\ &\lesssim h^{2\mu} (\|\mathbf{p}\|_{\mu, \mathcal{R}}^2 + \|\text{div } \mathbf{p}\|_{\mu, \mathcal{R}}^2) + h^2 \|\phi\|_{1, \mathcal{R}}^2 \\ &\lesssim h^{2\mu} \|S_f\|_{\mu, \mathcal{R}}^2. \end{aligned}$$

211

□

#### 212 4.5.2. Aubin-Nitsche-type estimates

213 To derive improved estimates on the error  $\|\phi - \phi_h\|_{0, \mathcal{R}}$  in  $\mathbf{X}_h = \mathbf{Q}_h^0 \times L_h^0$ , we shall rely on the illuminating  
 214 work of Falk-Osborn [18]. Interestingly, one can obtain an improvement of the convergence rate, contrary to the  
 215 case where the solution is “smooth”. From the previous analysis, for all  $\mu < r_{\max}$ , we already have the estimate  
 216 (4.22).

217 **Lemma 4.9.** *Let  $(\mathbf{p}, \phi)$  (resp.  $(\mathbf{p}_h, \phi_h)$ ) the solution of continuous (resp. discrete) variational problem (4.3)*  
 218 *(resp. (4.13)). For all  $(\mathbf{q}_h, \psi_h)$  in  $\mathbf{X}_h$ , it holds:*

$$a(\mathbf{p} - \mathbf{p}_h, \mathbf{q}_h) + b(\mathbf{q}_h, \phi - \phi_h) = 0, \quad (4.23)$$

219

$$b(\mathbf{p} - \mathbf{p}_h, \psi_h) + t(\phi - \phi_h, \psi_h) = 0. \quad (4.24)$$

220 *Proof.* Let  $(\mathbf{q}_h, \psi_h)$  be in  $\mathbf{X}_h$ . The subtraction of (4.3) from (4.13), with  $(\mathbf{q}, \psi) = (\mathbf{q}_h, \psi_h)$  in the former, gives

$$a(\mathbf{p} - \mathbf{p}_h, \mathbf{q}_h) + b(\mathbf{q}_h, \phi - \phi_h) + b(\mathbf{p} - \mathbf{p}_h, \psi_h) + t(\phi - \phi_h, \psi_h) = 0.$$

221 We obtain the first equality (4.23) (resp. the second equality (4.24)) with  $\psi_h = 0$  (resp.  $\mathbf{q}_h = \mathbf{0}$ ).  $\square$

222 Before improving the estimate, we need to introduce the adjoint problem:

223 For  $d \in L^2(\mathcal{R})$ , find  $(\mathbf{y}_d, \eta_d) \in \mathbf{X}$  such that  $\forall (\mathbf{q}, \psi) \in \mathbf{X}$ :

$$a(\mathbf{y}_d, \mathbf{q}) + b(\mathbf{q}, \eta_d) + b(\mathbf{y}_d, \psi) + t(\eta_d, \psi) = (d, \psi)_{0, \mathcal{R}}. \quad (4.25)$$

224 **Theorem 4.10.** *Under the assumptions of Proposition 3.1, it holds, with  $r_{\max} < 1/2$ :*

$$\forall \mu \in ]0, r_{\max}[, \forall S_f \in H^\mu(\mathcal{R}), \quad \|\phi - \phi_h\|_{0, \mathcal{R}} \lesssim h^{2\mu} \|S_f\|_{\mu, \mathcal{R}}. \quad (4.26)$$

225 *Proof.* Adapting the methodology of [18] and by using  $(0, \phi - \phi_h)$  as a test function in the adjoint problem  
226 (4.25), we remark:

$$\|\phi - \phi_h\|_{0, \mathcal{R}} = \sup_{d \in L^2(\mathcal{R}) \setminus \{0\}} \frac{b(\mathbf{y}_d, \phi - \phi_h) + t(\eta_d, \phi - \phi_h)}{\|d\|_{0, \mathcal{R}}}. \quad (4.27)$$

227 We now look for an upper bound of the supremum in (4.27). We find that the numerator is successively equal  
228 to:

$$b(\mathbf{y}_d - (\mathbf{y}_d)_R^0, \phi - \phi_h) + b((\mathbf{y}_d)_R^0, \phi - \phi_h) + t(\eta_d, \phi - \phi_h);$$

229 using (4.18), for any  $\psi_h^*, \psi_h'$  in  $L_h$ :

$$b(\mathbf{y}_d - (\mathbf{y}_d)_R^0, \phi - \psi_h^*) + b((\mathbf{y}_d)_R^0, \phi - \phi_h) + t(\eta_d - \psi_h', \phi - \phi_h) + t(\psi_h', \phi - \phi_h);$$

230 using (4.23) with  $\mathbf{q}_h = (\mathbf{y}_d)_R^0$ :

$$b(\mathbf{y}_d - (\mathbf{y}_d)_R^0, \phi - \psi_h^*) - a(\mathbf{p} - \mathbf{p}_h, (\mathbf{y}_d)_R^0) + t(\eta_d - \psi_h', \phi - \phi_h) + t(\psi_h', \phi - \phi_h);$$

231 now we use (4.24) with  $\psi_h = \psi_h'$ :

$$b(\mathbf{y}_d - (\mathbf{y}_d)_R^0, \phi - \psi_h^*) - a(\mathbf{p} - \mathbf{p}_h, (\mathbf{y}_d)_R^0) + t(\eta_d - \psi_h', \phi - \phi_h) - b(\mathbf{p} - \mathbf{p}_h, \psi_h');$$

232 we add (4.25) with  $(\mathbf{p} - \mathbf{p}_h, 0)$  as a test function:

$$b(\mathbf{y}_d - (\mathbf{y}_d)_R^0, \phi - \psi_h^*) + a(\mathbf{p} - \mathbf{p}_h, \mathbf{y}_d - (\mathbf{y}_d)_R^0) + t(\eta_d - \psi_h', \phi - \phi_h) + b(\mathbf{p} - \mathbf{p}_h, \eta_d - \psi_h'). \quad (4.28)$$

233 All terms<sup>1</sup> in the previous relation can be bounded with an  $h$ -dependent term:

$$\begin{aligned} \inf_{\psi_h^* \in L_h} |b(\mathbf{y}_d - (\mathbf{y}_d)_R^0, \phi - \psi_h^*)| &\lesssim \|\operatorname{div}(\mathbf{y}_d - (\mathbf{y}_d)_R^0)\|_{0, \mathcal{R}} \inf_{\psi_h^* \in L_h} \|\phi - \psi_h^*\|_{0, \mathcal{R}} \\ &\lesssim \|\operatorname{div} \mathbf{y}_d\|_{0, \mathcal{R}} h \|\phi\|_{1, \mathcal{R}} \\ &\lesssim h \|S_f\|_{\mu, \mathcal{R}} \|d\|_{0, \mathcal{R}}; \end{aligned}$$

<sup>1</sup>In particular,  $\|\operatorname{div}(\mathbf{y}_d - (\mathbf{y}_d)_R^0)\|_{0, \mathcal{R}} \lesssim \|\operatorname{div} \mathbf{y}_d\|_{0, \mathcal{R}}$  according to (4.15) and (4.19).

$$\begin{aligned}
 |a(\mathbf{p} - \mathbf{p}_h, \mathbf{y}_d - (\mathbf{y}_d)_R^0)| &\lesssim \|\mathbf{p} - \mathbf{p}_h\|_{0,\mathcal{R}} \|\mathbf{y}_d - (\mathbf{y}_d)_R^0\|_{0,\mathcal{R}} \\
 &\lesssim h^\mu \|S_f\|_{\mu,\mathcal{R}} (h^\mu \|\mathbf{y}_d\|_{\mu,\mathcal{R}} + h \|\operatorname{div} \mathbf{y}_d\|_{0,\mathcal{R}}) \\
 &\lesssim h^{2\mu} \|S_f\|_{\mu,\mathcal{R}} \|d\|_{0,\mathcal{R}}.
 \end{aligned}$$

234 The last two terms in (4.28) are considered together.

$$\begin{aligned}
 &\inf_{\psi'_h \in L_h} |b(\mathbf{p} - \mathbf{p}_h, \eta_d - \psi'_h) + t(\phi - \phi_h, \eta_d - \psi'_h)| \\
 &\lesssim (\|\operatorname{div}(\mathbf{p} - \mathbf{p}_h)\|_{0,\mathcal{R}} + \|\phi - \phi_h\|_{0,\mathcal{R}}) \inf_{\psi'_h \in L_h} \|\eta_d - \psi'_h\|_{0,\mathcal{R}} \\
 &\lesssim h^\mu \|S_f\|_{\mu,\mathcal{R}} \inf_{\psi'_h \in L_h} \|\eta_d - \psi'_h\|_{0,\mathcal{R}} \\
 &\lesssim h^\mu \|S_f\|_{\mu,\mathcal{R}} h \|\eta_d\|_{1,\mathcal{R}} \lesssim h^{\mu+1} \|S_f\|_{\mu,\mathcal{R}} \|d\|_{0,\mathcal{R}}.
 \end{aligned}$$

235 Thus, for low-regularity solutions ( $\mu < 1/2$ ), we conclude that it holds:

$$\|\phi - \phi_h\|_{0,\mathcal{R}} \lesssim \max(h, h^{2\mu}, h^{\mu+1}) \|S_f\|_{\mu,\mathcal{R}} \approx h^{2\mu} \|S_f\|_{\mu,\mathcal{R}}.$$

236

□

237 **Corollary 4.11.** *In the case of “smooth data”  $S_f$ , i.e.  $S_f \in H^{r_{\max}}(\mathcal{R})$ , the error estimate gives:*

$$\|\phi - \phi_h\|_{0,\mathcal{R}} \lesssim h^{2r_{\max}} \|S_f\|_{r_{\max},\mathcal{R}}.$$

## 238 4.6. Numerical analysis of the generalized eigenvalue problem

239 Let us focus on the approximation of the generalized eigenvalue problem (3.2) in our low-regularity setting,  
 240 under the assumptions of Proposition 3.1, supplemented with  $\underline{\nu}_{\Sigma_f} \in \mathcal{PW}^{1,\infty}(\mathcal{R})$ .

241 Let  $0 \leq \mu < r_{\max}$  be given, we introduce an operator  $B_\mu$  associated to the source problem (4.3): given  
 242  $f \in H^\mu(\mathcal{R})$ , we call  $B_\mu f = \phi \in H^1(\mathcal{R})$  the second component of the couple  $(\mathbf{p}, \phi)$  that solves (4.3) with source  
 243  $S_f = \underline{\nu}_{\Sigma_f} f$ . Since  $\underline{\nu}_{\Sigma_f}$  belongs to  $\mathcal{PW}^{1,\infty}(\mathcal{R})$ , it holds  $\|S_f\|_{\mu,\mathcal{R}} \lesssim \|f\|_{\mu,\mathcal{R}}$  because  $\mu < 1/2$ . Hence,  $B_\mu$  is a  
 244 bounded operator from  $H^\mu(\mathcal{R})$  to itself:

$$\|B_\mu f\|_{\mu,\mathcal{R}} \lesssim \|B_\mu f\|_{1,\mathcal{R}} = \|\phi\|_{1,\mathcal{R}} \lesssim \|S_f\|_{0,\mathcal{R}} \lesssim \|S_f\|_{\mu,\mathcal{R}} \lesssim \|f\|_{\mu,\mathcal{R}};$$

245 we write  $B_\mu \in \mathcal{L}(H^\mu(\mathcal{R}))$  for short. In addition, since the second component of the solution actually belongs  
 246 to  $H^1(\mathcal{R})$  with continuous dependence ( $\|\phi\|_{1,\mathcal{R}} \lesssim \|f\|_{\mu,\mathcal{R}}$ ), it follows that  $B_\mu$  is a compact operator. Denote by  
 247  $\sigma(B_\mu)$  its spectrum. By construction,  $\lambda^{-1} \in \sigma(B_\mu)$  if, and only if,  $\lambda$  is an eigenvalue of (3.2).

248 Finally, we consider the discrete operator  $B_\mu^h$  associated to the discrete source problem (4.13): given  $f \in$   
 249  $H^\mu(\mathcal{R})$ , we call  $B_\mu^h f$  the second component of the couple  $(\mathbf{p}_h, \phi_h)$  that solves (4.13) with source  $S_f = \underline{\nu}_{\Sigma_f} f$ .

250 Under the assumptions of Section 4.3 and as noted at the beginning of Section 4.5, it holds  $\lim_{h \rightarrow 0} \|B_0 f -$   
 251  $B_0^h f\|_{0,\mathcal{R}} = 0$  for all  $f \in L^2(\mathcal{R})$ . This property is the so-called pointwise convergence. However, for a mixed  
 252 formulation, the fact that the family  $(B_0^h)_h$  converges pointwise towards the compact operator  $B_0$  is not *sufficient*  
 253 to guarantee that the family  $(B_0^h)_h$  converges in operator norm towards  $B_0$ .

### 254 4.6.1. Convergence in operator norm

255 On the other hand, according to [27], proving that  $\lim_{h \rightarrow 0} \|B_\mu - B_\mu^h\|_{\mathcal{L}(H^\mu(\mathcal{R}))} = 0$  for discrete approximants  
 256  $(B_\mu^h)_h$  is a sufficient condition to obtain convergence of the eigenvalues. In order to ensure the convergence in  
 257 operator norm of the family  $(B_\mu^h)_h$  towards the compact operator  $B_\mu$ , we need a technical assumption on the  
 258 triangulations.

259 **Definition 4.12.** A family of triangulations  $(\mathcal{T}_h)_h$  is *regular<sup>+</sup>* if it satisfies:

$$\exists \theta > 0, \forall h, h^{2-\theta} \lesssim \min_{K \in \mathcal{T}_h} \text{diam}(K). \quad (4.29)$$

260 In particular, a quasi-uniform family of triangulations is *regular<sup>+</sup>* (take  $\theta = 1$  in (4.29)). For a *regular<sup>+</sup>* family,  
261 one has the following inverse inequality, whose proof is given in Appendix A.

262 **Lemma 4.13.** Let  $\mu \in [0, 1/2[$ . For a *regular<sup>+</sup>* family of triangulations, it holds:

$$\forall h, \forall \psi_h \in L_h^k, \|\psi_h\|_{\mu, \mathcal{R}} \lesssim h^{-2\mu+\theta\mu} \|\psi_h\|_{0, \mathcal{R}}. \quad (4.30)$$

263 **Theorem 4.14.** Under the assumptions of Proposition 3.1 with  $r_{\max} < 1/2$  plus  $\underline{\nu}_{\Sigma_f} \in \mathcal{PW}^{1, \infty}(\mathcal{R})$ , let  $\mu \in$   
264  $[0, r_{\max}[$ . Provided that the family of triangulations is *regular<sup>+</sup>*, one has:

$$\|B_\mu - B_\mu^h\|_{\mathcal{L}(H^\mu(\mathcal{R}))} \lesssim h^{\theta\mu}. \quad (4.31)$$

265 *Proof.* According to (4.26), we know that

$$\|(B_\mu - B_\mu^h)f\|_{0, \mathcal{R}} \lesssim h^{2\mu} \|f\|_{\mu, \mathcal{R}}. \quad (4.32)$$

266 It remains to estimate  $\|(B_\mu - B_\mu^h)f\|_{\mu, \mathcal{R}}$ : for that, we use the triangle inequality

$$\|(B_\mu - B_\mu^h)f\|_{\mu, \mathcal{R}} \leq \|B_\mu f - \pi^0(B_\mu f)\|_{\mu, \mathcal{R}} + \|\pi^0(B_\mu f) - B_\mu^h f\|_{\mu, \mathcal{R}}.$$

267 To bound the first term, we have according to Theorem 2.3 in [2] that

$$\forall \psi \in \mathcal{PH}^1(\mathcal{R}), \|\psi - \pi^0\psi\|_{\mu, \mathcal{R}} \lesssim h^{1-\mu} \|\psi\|_{\mathcal{PH}^1(\mathcal{R})}.$$

268 Applying the result to  $\psi = B_\mu f$ , we find  $\|B_\mu f - \pi^0(B_\mu f)\|_{\mu, \mathcal{R}} \lesssim h^{1-\mu} \|f\|_{\mu, \mathcal{R}}$ .

269 To bound the second term, we use first the inverse inequality (4.30) on the discrete space  $L_h^k$ , valid for a  
270 *regular<sup>+</sup>* family of triangulations. Applying the result to  $\psi_h = \pi^0(B_\mu f) - B_\mu^h f$  and using again the triangle  
271 inequality, we now find that

$$\begin{aligned} \|\pi^0(B_\mu f) - B_\mu^h f\|_{\mu, \mathcal{R}} &\lesssim h^{-2\mu+\theta\mu} \|\pi^0(B_\mu f) - B_\mu^h f\|_{0, \mathcal{R}} \\ &\lesssim h^{-2\mu+\theta\mu} (\|\pi^0(B_\mu f) - B_\mu f\|_{0, \mathcal{R}} + \|B_\mu f - B_\mu^h f\|_{0, \mathcal{R}}) \\ &\lesssim \max(h^{1-2\mu+\theta\mu}, h^{\theta\mu}) \|f\|_{\mu, \mathcal{R}}, \end{aligned}$$

272 where we have used (4.15) and (4.32) to derive the final estimate. Since  $\mu < 1/2$ , we conclude by aggregating  
273 the results that (4.31) holds.  $\square$

274 Thanks to [27], convergence of the discrete eigenvalues to the exact ones is guaranteed, and so is the absence  
275 of spectral pollution:

- 276 • Given any closed, non-empty disk  $D \subset \mathbb{C}$  such that  $D \cap \sigma(B_\mu) = \emptyset$ , there exists  $h_0 > 0$  such that, for all  
277  $h < h_0$ ,  $D \cap \sigma(B_\mu^h) = \emptyset$ .
- 278 • Given any closed, non-empty disk  $D \subset \mathbb{C}$  such that  $D \cap \sigma(B_\mu) = \{\lambda\}$ , with  $\lambda$  of multiplicity  $m_\lambda$ , there  
279 exists  $h_0 > 0$  such that, for all  $h < h_0$ ,  $D \cap \sigma(B_\mu^h)$  contains exactly  $m_\lambda$  discrete eigenvalues.

280 *4.6.2. Optimal convergence rate*

281 Let the assumptions of Theorem 4.14 hold. We determine now the rate of convergence of the eigenvalues in  
 282 the spirit of [8]. Let  $\nu = \lambda^{-1}$  be an eigenvalue of  $B_\mu$ . For simplicity, let us assume that  $\nu$  is a simple eigenvalue,  
 283 and denote by  $W$  the associated eigenspace. According to the absence of spectral pollution, for  $h$  small enough,  
 284 the closest discrete eigenvalue, denoted by  $\nu_h$ , is also simple; we denote by  $W_h$  the associated eigenspace.

285 **Definition 4.15.** Let  $\omega_\nu > 0$  be the regularity exponent of the eigenfunction, *i.e.* either  $W \subset \mathcal{P}H^{1+s}(\mathcal{R})$  for  
 286  $s < \omega_\nu$  and  $W \not\subset \mathcal{P}H^{1+\omega_\nu}(\mathcal{R})$ , or  $W \subset \mathcal{P}H^{1+\omega_\nu}(\mathcal{R})$  and  $W \not\subset \mathcal{P}H^{1+s}(\mathcal{R})$  for  $s > \omega_\nu$ . Let  $\omega = \min(\omega_\nu, m + 1)$ ,  
 287 where  $m \geq 0$  is the order of the RTN finite element.

288 Clearly,  $\omega_\nu$ , and as a consequence  $\omega$ , can be greater than  $r_{\max}$ . We shall prove that the approximation  
 289 converges with a rate equal to twice the exponent  $\omega$  defined above: this result is stated in Corollary 4.23 at the  
 290 end of the subsection.

291 Let  $\mu \in [0, r_{\max}[$  be given. As we defined  $B_\mu$  (resp.  $B_\mu^h$ ), we define  $A_\mu$  (resp.  $A_\mu^h$ ): for  $f \in H^\mu(\mathcal{R})$ , we call  
 292  $A_\mu f = \mathbf{p} \in \mathbf{H}(\text{div}, \mathcal{R})$  (resp.  $A_\mu^h f = \mathbf{p}_h \in \mathbf{Q}_h$ ) the first component of the couple  $(\mathbf{p}, \phi)$  (resp.  $(\mathbf{p}_h, \phi_h)$ ) that  
 293 solves (4.3) (resp. (4.13)) with source  $S_f = \underline{\nu}\Sigma_f f$ . The following lemma introduces some equalities that we will  
 294 use later on.

295 **Lemma 4.16.** *Let  $\varphi$  and  $\varphi'$  be given in  $W$ . Then, it holds:*

$$\begin{aligned} (\underline{\nu}\Sigma_f \varphi, (B_\mu - B_\mu^h)\varphi')_{0,\mathcal{R}} &= a(A_\mu \varphi, (A_\mu - A_\mu^h)\varphi') \\ &\quad + b((A_\mu - A_\mu^h)\varphi', B_\mu \varphi) + b(A_\mu \varphi, (B_\mu - B_\mu^h)\varphi') + t(B_\mu \varphi, (B_\mu - B_\mu^h)\varphi'); \end{aligned} \quad (4.33)$$

296 *and*

$$\begin{aligned} 0 &= a(A_\mu^h \varphi, (A_\mu - A_\mu^h)\varphi') + b((A_\mu - A_\mu^h)\varphi', B_\mu^h \varphi) \\ &\quad + b(A_\mu^h \varphi, (B_\mu - B_\mu^h)\varphi') + t(B_\mu^h \varphi, (B_\mu - B_\mu^h)\varphi'). \end{aligned} \quad (4.34)$$

297 *Proof.* The definitions of  $A_\mu, B_\mu$  imply that for all  $f \in H^\mu(\mathcal{R})$ , for all  $(\mathbf{q}, \psi) \in \mathbf{X}$ :

$$(\underline{\nu}\Sigma_f f, \psi)_{0,\mathcal{R}} = a(A_\mu f, \mathbf{q}) + b(\mathbf{q}, B_\mu f) + b(A_\mu f, \psi) + t(B_\mu f, \psi), \quad (4.35)$$

298 whereas the definitions of  $A_\mu^h, B_\mu^h$  imply that for all  $f \in H^\mu(\mathcal{R})$ , for all  $(\mathbf{q}, \psi) \in \mathbf{X}_h$ :

$$(\underline{\nu}\Sigma_f f, \psi)_{0,\mathcal{R}} = a(A_\mu^h f, \mathbf{q}) + b(\mathbf{q}, B_\mu^h f) + b(A_\mu^h f, \psi) + t(B_\mu^h f, \psi). \quad (4.36)$$

299 The first equality (4.33) comes from (4.35) with:

$$f = \varphi; \quad \mathbf{q} = (A_\mu - A_\mu^h)\varphi'; \quad \psi = (B_\mu - B_\mu^h)\varphi'.$$

300 The second one, (4.34), comes from the difference between (4.35) and (4.36) with:

$$f = \varphi'; \quad \mathbf{q} = A_\mu^h \varphi; \quad \psi = B_\mu^h \varphi;$$

301 and with the symmetry of  $a(\cdot, \cdot)$  and  $t(\cdot, \cdot)$ . □

302 We remark that  $\varphi \mapsto \|\varphi\|_W = \|(\underline{\nu}\Sigma_f)^{\frac{1}{2}}\varphi\|_{0,\mathcal{R}}$  is a norm over  $W$ ,<sup>2</sup> and this norm is induced by the inner  
303 product

$$(\varphi, \varphi')_W = (\underline{\nu}\Sigma_f\varphi, \varphi')_{0,\mathcal{R}}.$$

304 **Proposition 4.17.** *Let  $\omega$  be as in Definition 4.15. For every  $\varphi$  in  $W$ , the following inequalities hold:*

$$\begin{aligned} \|(B_\mu - B_\mu^h)\varphi\|_{0,\mathcal{R}} &\lesssim h^\omega \|\varphi\|_W \\ \|(A_\mu - A_\mu^h)\varphi\|_{\mathbf{H}(\text{div},\mathcal{R})} &\lesssim h^\omega \|\varphi\|_W. \end{aligned}$$

305 *Proof.* These two inequalities come from the first Strang's Lemma. The method is the same as for Theorem 4.7  
306 (see Rem. 4.8 for the "smooth" case). Here, we use the equivalence of all norms on  $W$  to state the result.  $\square$

307 Introducing  $\delta(Z, Z') = \sup_{z \in Z, \|z\|_0=1} \inf_{z' \in Z'} \|z - z'\|_{0,\mathcal{R}}$  for  $Z, Z'$  closed subspaces of  $L^2(\mathcal{R})$ , the gap between  
308  $W$  and  $W_h$  is defined by:

$$\hat{\delta}(W, W_h) = \max[\delta(W, W_h), \delta(W_h, W)],$$

309 It allows us to evaluate the approximation of the continuous eigenfunctions by their discrete counterparts.  
310 Classically, this gap can be bounded with the help of Proposition 4.17, following Theorem 1 from [27]:

$$\hat{\delta}(W, W_h) \lesssim h^\omega. \quad (4.37)$$

311 Let us now define  $E_h$  as the projector from  $L^2(\mathcal{R})$  onto  $W_h$  such that

$$\forall \varphi \in L^2(\mathcal{R}), \forall \psi_h \in W_h, (\underline{\nu}\Sigma_f(\varphi - E_h\varphi), \psi_h)_{0,\mathcal{R}} = 0. \quad (4.38)$$

312 **Lemma 4.18.** *The operators  $E_h$  and  $B_\mu^h$  commute.*

313 *Proof.* Let  $\varphi \in L^2(\mathcal{R})$  be decomposed into  $\varphi = E_h\varphi + \bar{\varphi}$ . By construction  $E_h\varphi \in W_h$ , so that  $B_\mu^h E_h\varphi \in W_h$ ,  
314 hence  $E_h B_\mu^h E_h\varphi = B_\mu^h E_h\varphi$  because  $W_h$  is invariant through  $E_h$ . It follows  $E_h B_\mu^h \varphi = E_h B_\mu^h E_h\varphi + E_h B_\mu^h \bar{\varphi} =$   
315  $B_\mu^h E_h\varphi + E_h B_\mu^h \bar{\varphi}$ . This is equivalently expressed as

$$(E_h B_\mu^h - B_\mu^h E_h)\varphi = E_h B_\mu^h \bar{\varphi}.$$

316 By construction,  $\psi_h = E_h B_\mu^h \bar{\varphi}$  belongs to  $W_h$ , with squared norm equal to

$$(\underline{\nu}\Sigma_f \psi_h, \psi_h)_{0,\mathcal{R}} = (\underline{\nu}\Sigma_f E_h B_\mu^h \bar{\varphi}, \psi_h)_{0,\mathcal{R}} = (\underline{\nu}\Sigma_f B_\mu^h \bar{\varphi}, \psi_h)_{0,\mathcal{R}} = (\underline{\nu}\Sigma_f \bar{\varphi}, B_\mu^h \psi_h)_{0,\mathcal{R}} = 0.$$

317 The penultimate equality stems from the fact that  $c(\cdot, \cdot)$  is symmetric, and the last one comes from the definition  
318 of  $\bar{\varphi}$  and  $E_h$ .  $\square$

319 Let  $F_h$  be the restriction of  $E_h$  to  $W$ . One has the following simple results as a consequence of the gap  
320 property.

321 **Lemma 4.19.** *For  $h$  small enough,  $F_h$  is a bijection from  $W$  to  $W_h$ . Moreover*

$$\forall \varphi \in W, \left\| (\underline{\nu}\Sigma_f)^{\frac{1}{2}}(\varphi - F_h\varphi) \right\|_{0,\mathcal{R}} \lesssim h^\omega \|\varphi\|_W. \quad (4.39)$$

<sup>2</sup>If  $\|\varphi\|_W = 0$ , then  $\underline{\nu}\Sigma_f\varphi = 0$ . By definition of  $W$ ,  $\varphi$  is solution of (3.2) with zero right-hand side. Thus, by uniqueness of the solution it follows that  $\varphi = 0$ .

322 Let  $\mathcal{S}_h = F_h^{-1}E_h - I \in \mathcal{L}(L^2(\mathcal{R}))$  for  $h$  small enough.

323 **Lemma 4.20.** *For  $h$  small enough,  $W \subset \ker(\mathcal{S}_h)$ ;  $(\mathcal{S}_h)_h$  is uniformly bounded.*

324 One can then prove an ‘‘orthogonality’’ result involving  $\mathcal{S}_h$ .

325 **Proposition 4.21.** *For all  $f$  in  $L^2(\mathcal{R})$  and  $\varphi_h$  in  $W_h$ , one has for  $h$  small enough*

$$(\underline{\nu}\Sigma_f \mathcal{S}_h f, \varphi_h)_{0,\mathcal{R}} = 0.$$

326 *Proof.* Let  $f$  be in  $L^2(\mathcal{R})$  and  $\varphi_h$  be in  $W_h$ . We find:

$$\begin{aligned} (\underline{\nu}\Sigma_f \mathcal{S}_h f, \varphi_h)_{0,\mathcal{R}} &= (\underline{\nu}\Sigma_f (F_h^{-1}E_h f - f), \varphi_h)_{0,\mathcal{R}} \\ &= (\underline{\nu}\Sigma_f (F_h^{-1}E_h f - E_h f), \varphi_h)_{0,\mathcal{R}} \\ &= (\underline{\nu}\Sigma_f (F_h^{-1}E_h f - F_h F_h^{-1}E_h f), \varphi_h)_{0,\mathcal{R}}. \end{aligned}$$

327 The second equality uses (4.38) with  $\varphi = f$ . One concludes by remarking that  $\psi = F_h^{-1}E_h f \in W$  so  $(\underline{\nu}\Sigma_f (\psi -$   
328  $F_h \psi), \varphi_h)_{0,\mathcal{R}} = 0$  using again (4.38), because  $F_h \psi = E_h \psi$ .

329 □

330 To obtain an optimal rate of convergence we restrict the operators  $B_\mu$  and  $B_\mu^h$  to the eigenspace  $W$ . We denote  
331 finally by  $\hat{B}_\mu$  and  $\hat{B}_\mu^h$  the operators, from  $W$  to itself,  $\hat{B}_\mu = B_\mu|_W$  and  $\hat{B}_\mu^h = F_h^{-1}B_\mu^h F_h$ . Let us estimate

$$\|\hat{B}_\mu - \hat{B}_\mu^h\|_{\mathcal{L}(W)} = \sup_{\varphi, \varphi' \in W \setminus \{0\}} \frac{|(\varphi, (\hat{B}_\mu - \hat{B}_\mu^h)\varphi')_W|}{\|\varphi\|_W \|\varphi'\|_W}.$$

332 **Theorem 4.22.** *Let  $\omega$  be as in Definition 4.15. Then for  $h$  small enough, the following estimate holds true*

$$\|\hat{B}_\mu - \hat{B}_\mu^h\|_{\mathcal{L}(W)} \lesssim h^{2\omega}. \quad (4.40)$$

333 *Proof.* Using the definition of  $F_h$ , Lemma 4.18 and finally Lemma 4.20, one checks that for all  $\varphi' \in W$ :

$$\begin{aligned} (\hat{B}_\mu - \hat{B}_\mu^h)\varphi' &= B_\mu \varphi' - F_h^{-1}B_\mu^h F_h \varphi' \\ &= B_\mu \varphi' - F_h^{-1}B_\mu^h E_h \varphi' \\ &= B_\mu \varphi' - F_h^{-1}E_h B_\mu^h \varphi' \\ &= (B_\mu - B_\mu^h)\varphi' + B_\mu^h \varphi' - F_h^{-1}E_h B_\mu^h \varphi' + \mathcal{S}_h B_\mu \varphi' \\ &= (B_\mu - B_\mu^h)\varphi' + \mathcal{S}_h (B_\mu - B_\mu^h)\varphi'. \end{aligned} \quad (4.41)$$

334 Hence, given  $\varphi, \varphi' \in W$ , we can bound  $|(\varphi, (\hat{B}_\mu - \hat{B}_\mu^h)\varphi')_W| = |(\underline{\nu}\Sigma_f \varphi, (\hat{B}_\mu - \hat{B}_\mu^h)\varphi')_{0,\mathcal{R}}|$  by

$$|(\underline{\nu}\Sigma_f \varphi, (B_\mu - B_\mu^h)\varphi')_{0,\mathcal{R}}| + |(\underline{\nu}\Sigma_f \varphi, \mathcal{S}_h (B_\mu - B_\mu^h)\varphi')_{0,\mathcal{R}}|.$$

335 Let us bound each part separately below.

336 One obtains from the difference between (4.33) and (4.34)

$$\begin{aligned} (\underline{\nu}\Sigma_f \varphi, (B_\mu - B_\mu^h)\varphi')_{0,\mathcal{R}} &= a((A_\mu - A_\mu^h)\varphi, (A_\mu - A_\mu^h)\varphi') + b((A_\mu - A_\mu^h)\varphi', (B_\mu - B_\mu^h)\varphi) \\ &\quad + b((A_\mu - A_\mu^h)\varphi, (B_\mu - B_\mu^h)\varphi') + t((B_\mu - B_\mu^h)\varphi, (B_\mu - B_\mu^h)\varphi'). \end{aligned}$$

337 Then, one can bound the first part:

$$\begin{aligned}
|(\underline{\nu}\Sigma_f\varphi, (B_\mu - B_\mu^h)\varphi')_{0,\mathcal{R}}| &\lesssim \|(A_\mu - A_\mu^h)\varphi\|_{0,\mathcal{R}}\|(A_\mu - A_\mu^h)\varphi'\|_{0,\mathcal{R}} \\
&\quad + \|\operatorname{div}(A_\mu - A_\mu^h)\varphi'\|_{0,\mathcal{R}}\|(B_\mu - B_\mu^h)\varphi\|_{0,\mathcal{R}} \\
&\quad + \|\operatorname{div}(A_\mu - A_\mu^h)\varphi\|_{0,\mathcal{R}}\|(B_\mu - B_\mu^h)\varphi'\|_{0,\mathcal{R}} \\
&\quad + \|(B_\mu - B_\mu^h)\varphi\|_{0,\mathcal{R}}\|(B_\mu - B_\mu^h)\varphi'\|_{0,\mathcal{R}} \\
&\lesssim h^{2\omega}\|\varphi\|_W\|\varphi'\|_W.
\end{aligned}$$

338 The second part is bounded by:

$$\begin{aligned}
|(\underline{\nu}\Sigma_f\varphi, \mathcal{S}_h(B_\mu - B_\mu^h)\varphi')_{0,\mathcal{R}}| &= |(\underline{\nu}\Sigma_f(\varphi - F_h\varphi), \mathcal{S}_h(B_\mu - B_\mu^h)\varphi')| \\
&\leq \|\underline{\nu}\Sigma_f(\varphi - F_h\varphi)\|_{0,\mathcal{R}}\|\mathcal{S}_h(B_\mu - B_\mu^h)\varphi'\|_{0,\mathcal{R}} \\
&\lesssim \|\underline{\nu}\Sigma_f(\varphi - F_h\varphi)\|_{0,\mathcal{R}}\|(B_\mu - B_\mu^h)\varphi'\|_{0,\mathcal{R}} \\
&\lesssim h^{2\omega}\|\varphi\|_W\|\varphi'\|_W.
\end{aligned}$$

339 In the first line we use Proposition 4.21 with  $f = (B_\mu - B_\mu^h)\varphi'$  and  $\varphi_h = F_h\varphi$ . In the third line we use the  
340 uniform continuity of  $\mathcal{S}_h$  in  $h$ , and in the last line we use the first inequality of Proposition 4.17 and the  
341 estimation (4.39). Therefore we have obtained (4.40).  $\square$

342 From this estimation and the work of Osborn in Theorem 2 of [27], one derives an optimal estimate on the error  
343 on the eigenvalues.

344 **Corollary 4.23.** *Let  $\omega$  be as in Definition 4.15. Then for  $h$  small enough, the error on the eigenvalue is given*  
345 *by*

$$|\nu - \nu_h| \lesssim h^{2\omega}.$$

346 **Remark 4.24.** If  $\nu$  has an algebraic multiplicity  $m_\nu > 1$ , the previous analysis and the *a priori* estimate are  
347 still valid with  $\nu_h = \frac{1}{m_\nu} \sum_{i=1}^{m_\nu} \nu_{h,i}$ , where  $(\nu_{h,i})_{i=1, \dots, m_\nu}$  are the  $m$  discrete eigenvalues closest to  $\nu$ , see again  
348 Theorem 2 of [27].

## 349 5. THE DD CASE

350 We continue by considering the neutron diffusion problem using a domain decomposition method: we call  
351 it the DD case. The diffusion problem with low-regularity solution in a mixed, multi-domain form has been  
352 analyzed in [13]. In this section, we first define some notations and spaces. Then we recall some results of [13],  
353 in which technical aspects on the choice and properties of the spaces and discretization are discussed. Finally,  
354 we define the variational formulation. The numerical analysis of the DD case is carried out in Section 6.

### 355 5.1. Setting of the DD spaces

356 Let us consider a partition  $\{\tilde{\mathcal{R}}_i\}_{1 \leq i \leq \tilde{N}}$  of  $\mathcal{R}$  which can be independent from the physical partition of the  
357 materials in  $\mathcal{R}$  (see e.g. [10, 11, 23]). In other words, it can happen that  $\{\tilde{\mathcal{R}}_i\}_{1 \leq i \leq \tilde{N}} \neq \{\mathcal{R}_i\}_{1 \leq i \leq N}$ . We denote  
358 by  $\Gamma_{ij}$  the interface between two subdomains  $\tilde{\mathcal{R}}_i$  and  $\tilde{\mathcal{R}}_j$ , for  $i \neq j$ : if the Hausdorff dimension of  $\tilde{\mathcal{R}}_i \cap \tilde{\mathcal{R}}_j$  is  
359  $d - 1$ , then  $\Gamma_{ij} = \operatorname{int}(\tilde{\mathcal{R}}_i \cap \tilde{\mathcal{R}}_j)$ ; otherwise,  $\Gamma_{ij} = \emptyset$ . By construction,  $\Gamma_{ij} = \Gamma_{ji}$ . We define the interface  $\Gamma_S$ ,



360 respectively the wirebasket  $\partial\Gamma_W$  by

$$\Gamma_S = \bigcup_{i=1}^{\tilde{N}} \bigcup_{j=i+1}^{\tilde{N}} \overline{\Gamma_{ij}}, \quad \partial\Gamma_W = \bigcup_{i=1}^{\tilde{N}} \bigcup_{j=i+1}^{\tilde{N}} \partial\Gamma_{ij}.$$

361 It is stressed that the resulting interface  $\Gamma_S$  needs not necessarily coincide with the physical interface between  
362 cells.

363 When  $d = 2$ , the wirebasket consists of isolated crosspoints. When  $d = 3$ , the wirebasket consists of open  
364 edges and crosspoints. For a field  $v$  defined over  $\mathcal{R}$ , we shall use the notation  $v_i = v|_{\tilde{\mathcal{R}}_i}$ , for  $1 \leq i \leq \tilde{N}$ . Let us  
365 define the function space with zero Dirichlet boundary condition:

$$\tilde{\mathcal{P}}H_0^1(\mathcal{R}) = \left\{ \psi \in L^2(\mathcal{R}) \mid \psi_i \in H^1(\tilde{\mathcal{R}}_i), \psi|_{\partial\tilde{\mathcal{R}}_i \setminus \Gamma_S} = 0, 1 \leq i \leq \tilde{N} \right\}.$$

When  $\Gamma_{ij} \neq \emptyset$ , let  $H_{\Gamma_{ij}}^{1/2}$  be the set of  $H^{1/2}(\Gamma_{ij})$  functions whose continuation by 0 to  $\partial\mathcal{R}_i$  belongs to  $H^{1/2}(\partial\mathcal{R}_i)$ .  
On can prove that  $H_{\Gamma_{ij}}^{1/2} = H_{\Gamma_{ji}}^{1/2}$ . We also introduce the space of piecewise  $\mathbf{H}(\text{div})$  vector-valued functions:

$$\tilde{\mathcal{P}}\mathbf{H}(\text{div}, \mathcal{R}) = \left\{ \mathbf{q} \in \mathbf{L}^2(\mathcal{R}) \mid \mathbf{q}_i \in \mathbf{H}(\text{div}, \tilde{\mathcal{R}}_i), 1 \leq i \leq \tilde{N} \right\}, \quad \|\mathbf{q}\|_{\tilde{\mathcal{P}}\mathbf{H}(\text{div}, \mathcal{R})} = \left( \sum_i \|\mathbf{q}_i\|_{\mathbf{H}(\text{div}, \tilde{\mathcal{R}}_i)}^2 \right)^{1/2}.$$

366 For  $\mathbf{p} \in \tilde{\mathcal{P}}\mathbf{H}(\text{div}, \mathcal{R})$ , let us set  $[\mathbf{p} \cdot \mathbf{n}]_{ij} := \sum_{k=i,j} \mathbf{p}_k \cdot \mathbf{n}_k|_{\Gamma_{ij}}$  the jump of the normal component of  $\mathbf{p}$  on  $\Gamma_{ij}$   
367 when  $\Gamma_{ij} \neq \emptyset$ .  $[\mathbf{p} \cdot \mathbf{n}]_{ij}$  is well defined in  $(H_{\Gamma_{ij}}^{1/2})'$  the dual space of  $H_{\Gamma_{ij}}^{1/2}$  (see *e.g.* [19]). The *global jump*  $[\mathbf{p} \cdot \mathbf{n}]$  of  
368 the normal component on the interface is defined by:

$$[\mathbf{p} \cdot \mathbf{n}]_{|\Gamma_{ij}} := [\mathbf{p} \cdot \mathbf{n}]_{ij}, \quad \text{for } 1 \leq i, j \leq \tilde{N}.$$

369 By definition, it holds  $[\mathbf{p} \cdot \mathbf{n}] \in \prod_{i < j} (H_{\Gamma_{ij}}^{1/2})'$ . We recall that for  $\mathbf{p} \in \mathbf{H}(\text{div}, \mathcal{R})$ , the global jump vanishes:  
370  $[\mathbf{p} \cdot \mathbf{n}] = 0$  (see *e.g.* [13], Lem. 1).

371 We introduce finally the following Hilbert spaces:

$$\begin{aligned} M &= \left\{ \psi_S \in \prod_{i < j} L^2(\Gamma_{ij}) \right\}, \quad \|\psi_S\|_M = \left( \sum_{i < j} \|\psi_S\|_{0, \Gamma_{ij}}^2 \right)^{1/2}; \\ H_-^{1/2}(\Gamma_S) &= \left\{ \psi_S \in M \mid \psi_S|_{\Gamma_{ij}} \in H^{1/2}(\Gamma_{ij}), \forall i < j \right\}, \quad \text{with graph norm}; \\ \tilde{\mathbf{Q}} &= \left\{ \mathbf{q} \in \tilde{\mathcal{P}}\mathbf{H}(\text{div}, \mathcal{R}) \mid [\mathbf{q} \cdot \mathbf{n}] \in M \right\}, \\ \|\mathbf{q}\|_{\tilde{\mathbf{Q}}} &= \left( \|\mathbf{q}\|_{\tilde{\mathcal{P}}\mathbf{H}(\text{div}, \mathcal{R})}^2 + \|[\mathbf{q} \cdot \mathbf{n}]\|_M^2 \right)^{1/2}; \\ \tilde{\mathbf{X}} &= \left\{ \xi := (\mathbf{q}, \psi) \in \tilde{\mathbf{Q}} \times L^2(\mathcal{R}) \right\}, \quad \|\xi\|_{\tilde{\mathbf{X}}} := \left( \|\mathbf{q}\|_{\tilde{\mathbf{Q}}}^2 + \|\psi\|_{0, \mathcal{R}}^2 \right)^{1/2}; \\ \tilde{\mathbf{W}} &= \left\{ \mathbf{w} := (\xi, \psi_S) \in \tilde{\mathbf{X}} \times M \right\}, \quad \|\mathbf{w}\|_{\tilde{\mathbf{W}}} := \left( \|\xi\|_{\tilde{\mathbf{X}}}^2 + \|\psi_S\|_M^2 \right)^{1/2}. \end{aligned}$$

372 By construction, one has  $M \subset \prod_{i < j} (H_{\Gamma_{ij}}^{1/2})'$ . We will next define a variational formulation which is conforming  
373 in  $\tilde{\mathbf{Q}} \times L^2(\mathcal{R})$ .

## 5.2. Variational formulation and discretization in the DD case

The mixed form of the neutron diffusion problem (4.1) is now given by (see Sect. 3.2 from [13]):

Find  $(\mathbf{p}, \phi, \phi_S) \in \tilde{\mathbf{Q}} \times \tilde{\mathcal{P}}H_0^1(\mathcal{R}) \times M$  such that:

$$\begin{cases} -D_i^{-1} \mathbf{p}_i - \mathbf{grad} \phi_i = 0 & \text{in } \tilde{\mathcal{R}}_i, \quad \text{for } 1 \leq i \leq \tilde{N}, \\ \operatorname{div} \mathbf{p}_i + \Sigma_{a,i} \phi_i = S_{f,i} & \text{in } \tilde{\mathcal{R}}_i, \quad \text{for } 1 \leq i \leq \tilde{N}, \\ \phi_i = \phi_S & \text{on } \partial \tilde{\mathcal{R}}_i \cap \Gamma_S, \quad \text{for } 1 \leq i \leq \tilde{N}, \\ [\mathbf{p} \cdot \mathbf{n}] = 0 & \text{on } \Gamma_S. \end{cases} \quad (5.1)$$

To solve this problem, we are looking for a solution  $((\mathbf{p}, \phi), \phi_S)$  in  $\mathbb{W}$ . Find  $((\mathbf{p}, \phi), \phi_S) \in \mathbb{W}$ , such that  $\forall ((\mathbf{q}, \psi), \psi_S) \in \mathbb{W}$ :

$$\int_{\mathcal{R}} (-D^{-1} \mathbf{p} \cdot \mathbf{q} + \phi \operatorname{div} \mathbf{q} + \psi \operatorname{div} \mathbf{p} + \Sigma_a \phi \psi) + \int_{\Gamma_S} [\mathbf{p} \cdot \mathbf{n}] \psi_S - \int_{\Gamma_S} [\mathbf{q} \cdot \mathbf{n}] \phi_S = \int_{\mathcal{R}} S_f \psi. \quad (5.2)$$

In (5.1)–(5.2),  $\phi_S, \psi_S$  play the role of Lagrange multipliers, with  $M$  the space of those Lagrange multipliers. To be mathematically precise, we should be integrating on  $\cup_{i < j} \Gamma_{ij}$  instead of  $\Gamma_S$ . We make this slight abuse of notations from now on. This approach is called the DD+ $L^2$ -jumps method.

From now on, we use the notations:

- $\mathbf{u} = (\zeta, \phi_S)$ ,  $\zeta = (\mathbf{p}, \phi)$ ,  $\mathbf{p} = (\mathbf{p}_i)_{1 \leq i \leq \tilde{N}}$  and  $\phi = (\phi_i)_{1 \leq i \leq \tilde{N}}$ ;
- $\mathbf{w} = (\xi, \psi_S)$ ,  $\xi = (\mathbf{q}, \psi)$ ,  $\mathbf{q} = (\mathbf{q}_i)_{1 \leq i \leq \tilde{N}}$  and  $\psi = (\psi_i)_{1 \leq i \leq \tilde{N}}$ ;

and we define the bilinear forms:

$$\ell_S : \begin{cases} \mathbb{W} \times \mathbb{W} \rightarrow \mathbb{R} \\ (\mathbf{u}, \mathbf{w}) \mapsto \int_{\Gamma_S} [\mathbf{p} \cdot \mathbf{n}] \psi_S \end{cases}, \quad (5.3)$$

and:

$$c_S : \begin{cases} \mathbb{W} \times \mathbb{W} \rightarrow \mathbb{R} \\ (\mathbf{u}, \mathbf{w}) \mapsto c(\zeta, \xi) + \ell_S(\mathbf{u}, \mathbf{w}) - \ell_S(\mathbf{w}, \mathbf{u}) \end{cases}. \quad (5.4)$$

We consider the linear form:

$$f_S : \begin{cases} \mathbb{W} \rightarrow \mathbb{R} \\ \mathbf{w} \mapsto f(\xi) \end{cases}. \quad (5.5)$$

Above, we extended the definition (4.7) (resp. (4.8)) of the form  $c$  (resp.  $f$ ), to elements of  $\tilde{\mathbf{X}} \times \tilde{\mathbf{X}}$  (resp.  $\tilde{\mathbf{X}}$ ). We may rewrite the variational formulation (5.2) as:

Find  $\mathbf{u} \in \mathbb{W}$  such that  $\forall \mathbf{w} \in \mathbb{W}$ :

$$c_S(\mathbf{u}, \mathbf{w}) = f_S(\mathbf{w}). \quad (5.6)$$

We recall that  $c_S$  satisfies an inf-sup condition, so the variational problem is well-posed (see [13], Sect. 4), and that, under the assumptions of Proposition 3.1, the global jump of  $\mathbf{p}$  vanishes:  $[\mathbf{p} \cdot \mathbf{n}] = 0$  in  $M$  (see Lem. 1 of [13]).

We study abstract, conforming, discretization of the variational formulation (5.6) as it is done in Section 5 from

395 [13]. To that aim, we introduce discrete, finite-dimensional, spaces indexed by a (small) parameter  $h$  as follows:  
 396  $\mathbf{Q}_{i,h} \subset \mathbf{H}(\operatorname{div}, \tilde{\mathcal{R}}_i)$  and  $L_{i,h} \subset L^2(\tilde{\mathcal{R}}_i)$ , for  $1 \leq i \leq \tilde{N}$ . We impose the following requirements, for all  $1 \leq i \leq \tilde{N}$ :

- 397 •  $\mathbf{q}_{i,h} \cdot \mathbf{n}|_{\partial\tilde{\mathcal{R}}_i} \in L^2(\partial\tilde{\mathcal{R}}_i)$  for all  $h > 0$ , for all  $\mathbf{q}_{i,h} \in \mathbf{Q}_{i,h}$ ;
- 398 •  $\operatorname{div} \mathbf{Q}_{i,h} \subset L_{i,h}$  for all  $h > 0$ ;
- 399 •  $(\mathbf{Q}_{i,h})_h$  and  $(L_{i,h})_h$  satisfy the *approximability property* (4.12) in  $\tilde{\mathcal{R}}_i$ .

400 Then, let

$$\tilde{\mathbf{Q}}_h = \prod_{1 \leq i \leq \tilde{N}} \mathbf{Q}_{i,h} \quad \text{and} \quad L_h = \prod_{1 \leq i \leq \tilde{N}} L_{i,h}.$$

401 In particular, the discretization  $\tilde{\mathbf{Q}}_h \times L_h$  is globally conforming in  $\tilde{\mathbf{Q}} \times L^2(\mathcal{R})$ . We endow  $\tilde{\mathbf{Q}}_h$  with the norm  
 402  $\|\cdot\|_{\tilde{\mathbf{Q}}}$ , while  $L_h$  is endowed with  $\|\cdot\|_{0,\mathcal{R}}$ .

403 We then define  $T_{i,h}$  as the space of the normal traces of vectors of  $\mathbf{Q}_{i,h}$  on  $\partial\tilde{\mathcal{R}}_i \cap \Gamma_S$ :

$$T_{i,h} := \left\{ q_{i,h} \in L^2(\partial\tilde{\mathcal{R}}_i \cap \Gamma_S) \mid \exists \mathbf{q}_{i,h} \in \mathbf{Q}_{i,h}, q_{i,h} = \mathbf{q}_{i,h} \cdot \mathbf{n}|_{\partial\tilde{\mathcal{R}}_i \cap \Gamma_S} \right\}. \quad (5.7)$$

404 Classically, several situations can occur on a given interface  $\Gamma_{ij}$ ,  $1 \leq i, j \leq \tilde{N}$ :

- 405 (1) *non-nested meshes*:  $T_{i,h}|_{\Gamma_{ij}} \not\subset T_{j,h}|_{\Gamma_{ij}}$  and  $T_{j,h}|_{\Gamma_{ij}} \not\subset T_{i,h}|_{\Gamma_{ij}}$ ;
- 406 (2) *nested meshes*:  $T_{i,h}|_{\Gamma_{ij}} \subset T_{j,h}|_{\Gamma_{ij}}$  or  $T_{j,h}|_{\Gamma_{ij}} \subset T_{i,h}|_{\Gamma_{ij}}$ ;
- 407 (3) *matching meshes*: nested meshes with  $T_{i,h}|_{\Gamma_{ij}} = T_{j,h}|_{\Gamma_{ij}}$ .

408 Usually, the term *nested meshes* is used to describe a family of successively refined meshes. In this paper, we  
 409 will use this expression to express that on all interfaces  $\Gamma_{ij}$ , case (5.2) described above holds. As an illustration,  
 410 see the interfaces between the subdomains in Fig. 3a.

411 Let us denote by  $M_h \subset M$  the discrete space of the Lagrange multipliers. We assume that  $M_h$  includes the  
 412 subspace  $M_h^0$  of piecewise constant fields. We introduce the discrete projection operators ([13], Sect. 5) from  
 413 the spaces of normal traces  $T_{i,h}$  to  $M_h$ , and vice versa, which are defined by:

$$\forall q_{i,h} \in T_{i,h}, \forall \psi_{S,h} \in M_h \left\{ \begin{array}{l} \int_{\partial\tilde{\mathcal{R}}_i \cap \Gamma_S} (\Pi_i(q_{i,h}) - q_{i,h}) \psi_{S,h} = 0 \\ \int_{\partial\tilde{\mathcal{R}}_i \cap \Gamma_S} (\pi_i(\psi_{S,h}) - \psi_{S,h}) q_{i,h} = 0 \end{array} \right. . \quad (5.8)$$

414 As the operators  $\Pi_i$  and  $\pi_i$  are orthogonal projections, they are continuous, with a continuity modulus equal  
 415 to 1. We also introduce the orthogonal projection operator  $\Pi_S^0 : M \rightarrow M_h^0$ . According to Proposition 1.135 of  
 416 [17], if we denote by  $h_S$  the meshsize on  $\Gamma_S$ :

$$\forall \psi_S \in H_-^{1/2}(\Gamma_S), \|\psi_S - \Pi_S^0(\psi_S)\|_M \lesssim h_S^{1/2} \|\psi_S\|_{H_-^{1/2}(\Gamma_S)}. \quad (5.9)$$

417 Next, let  $\mathbf{p}_h \in \tilde{\mathbf{Q}}_h$ . We define the discrete jump of the normal component of  $\mathbf{p}_h$  on the interface  $\Gamma_{ij}$  as  $[\mathbf{p}_h \cdot$   
 418  $\mathbf{n}]_{h,ij} := \sum_{l=i,j} \Pi_l(\mathbf{p}_{l,h} \cdot \mathbf{n}|_{\Gamma_{ij}})$ . The discrete global jump of the normal component,  $[\mathbf{p}_h \cdot \mathbf{n}]_h \in M_h$ , is defined by:

$$[\mathbf{p}_h \cdot \mathbf{n}]_{h|\Gamma_{ij}} := [\mathbf{p}_h \cdot \mathbf{n}]_{h,ij}, \quad \text{for } 1 \leq i, j \leq \tilde{N}.$$

419 We finally define:

$$\begin{aligned}\tilde{\mathbf{X}}_h &= \left\{ \xi_h := (\mathbf{q}_h, \psi_h) \in \tilde{\mathbf{Q}}_h \times L_h \right\}, \text{ endowed with } \|\cdot\|_{\tilde{\mathbf{X}}}, \\ \mathbf{W}_h &= \left\{ \mathbf{w}_h := (\xi_h, \psi_{S,h}) \in \tilde{\mathbf{X}}_h \times M_h \right\}, \text{ endowed with } \|\cdot\|_{\mathbf{W}}.\end{aligned}$$

420 In the DD+ $L^2$ -jumps setting, the conforming discretization of the variational formulation (5.6) reads:

$$\text{Find } \mathbf{u}_h \in \mathbf{W}_h \text{ such that } \forall \mathbf{w}_h \in \mathbf{W}_h, \quad c_S(\mathbf{u}_h, \mathbf{w}_h) = f_S(\mathbf{w}_h). \quad (5.10)$$

421 It is shown in Section 5 from [13] that  $c_S$  verifies a discrete inf-sup condition if the following conditions hold:

$$\exists \beta_h > 0, \forall \mathbf{q}_h \in \tilde{\mathbf{Q}}_h, \quad \int_{\Gamma_S} [\mathbf{q}_h \cdot \mathbf{n}]_h [\mathbf{q}_h \cdot \mathbf{n}] \geq \beta_h \int_{\Gamma_S} [\mathbf{q}_h \cdot \mathbf{n}]^2 \quad (5.11)$$

422 and

$$\begin{aligned}\exists \gamma_h > 0, \quad \forall \psi_{S,h} \in M_h, \\ \sum_{i=1}^{\tilde{N}} \sum_{j=i+1}^{\tilde{N}} \int_{\Gamma_{ij}} (\pi_i(\psi_{S,h})^2 + \pi_j(\psi_{S,h})^2) \geq \gamma_h \|\psi_{S,h}\|_M^2,\end{aligned} \quad (5.12)$$

423 Moreover, if  $\beta_h$  and  $\gamma_h$  can be chosen independently of  $h$ , the form  $c_S$  satisfies a udisc. For instance, conditions  
424 (5.11)–(5.12) are uniformly fulfilled when  $M_h$  is chosen as

$$M_h = \sum_{i=1}^{\tilde{N}} T_{i,h}. \quad (5.13)$$

425 Last, under (5.11), one easily checks that  $[\mathbf{p}_h \cdot \mathbf{n}] = 0$ . In other words:

$$\mathbf{p}_h \in \mathbf{H}(\text{div}, \mathcal{R}) \cap \tilde{\mathbf{Q}}_h. \quad (5.14)$$

426 In the DD case, we define  $\mathbf{Q}_h = \mathbf{H}(\text{div}, \mathcal{R}) \cap \tilde{\mathbf{Q}}_h$ .

## 427 6. NUMERICAL ANALYSIS IN THE DD CASE

428 To carry out the numerical analysis in the low-regularity case, we first introduce a suitable discretization  
429 of the DD problem, and then we carry out the numerical analysis on this discretization. Again, if one chooses  
430 another discretization that fulfills those properties detailed in the previous section, one may recover similar  
431 convergence results.

### 432 6.1. Discretization

433 We consider (5.10) where the RTN finite element is used on each subdomain with a conforming mesh, or  
434 triangulation. For  $1 \leq i \leq \tilde{N}$ , let  $h_i$  denote the local meshsize in  $\tilde{\mathcal{R}}_i$ , and  $h = \max_i h_i$  the global meshsize. Let  
435 us denote by  $k_i \geq 0$  the order of the discretization in  $\tilde{\mathcal{R}}_i$ , and  $k = \min_i k_i$ , the minimal order of the RTN finite  
436 element. The local RTN finite element subspace of  $\mathbf{H}(\text{div}, \tilde{\mathcal{R}}_i) \times L^2(\tilde{\mathcal{R}}_i)$  is defined as  $\mathbf{Q}_{i,h_i}^{k_i} \times L_{i,h_i}^{k_i}$ . With this  
437 choice, we have  $\text{div } \mathbf{Q}_{i,h_i}^{k_i} \subset L_{i,h_i}^{k_i}$  as required: local consistency is ensured. Now, if we set  $\tilde{\mathbf{Q}}_h^k = \prod_{1 \leq i \leq \tilde{N}} \mathbf{Q}_{i,h_i}^{k_i}$   
438 and  $L_h^k = \prod_{1 \leq i \leq \tilde{N}} L_{i,h_i}^{k_i}$ , we have  $\mathbf{q}_{i,h} \cdot \mathbf{n}|_{\partial \tilde{\mathcal{R}}_i} \in L^2(\partial \tilde{\mathcal{R}}_i)$  for all  $\mathbf{q}_{i,h} \in \mathbf{Q}_{i,h_i}^{k_i}$ , hence it follows that  $\tilde{\mathbf{Q}}_h^k \subset \mathbf{Q}$ :

439 the discretization  $\tilde{\mathbf{Q}}_h^k \times L_h^k$  is globally conforming in  $\tilde{\mathbf{Q}} \times L^2(\mathcal{R})$ . For the reader's convenience, we omit the  
 440 superscript  $k_i$  in the analysis below.

441 Finally, we choose  $M_h$  so that on the one hand (5.11)–(5.12) hold uniformly, and on the other hand it holds  
 442  $h_S \lesssim h$ : we refer to Section 5.2 from [13] for an extended discussion on suitable choices. According to the first  
 443 Strang's Lemma [17] and because  $c_S$  verifies a udisc, the error reads:

$$\|\mathbf{u} - \mathbf{u}_h\|_{\mathbb{W}} \lesssim \inf_{\mathbf{w}_h \in \mathbb{W}_h} \|\mathbf{u} - \mathbf{w}_h\|_{\mathbb{W}}. \quad (6.1)$$

444 As a consequence  $\lim_{h \rightarrow 0} \|\mathbf{u} - \mathbf{u}_h\|_{\mathbb{W}} = 0$ . This result holds for nested and non-nested meshes. We study below  
 445 how to improve the bound on the error, how to derive an Aubin-Nitsche estimate, and finally how to prove  
 446 convergence for the generalized eigenvalue problem, for *nested* meshes.<sup>3</sup> As previously, those results hold under  
 447 the assumptions of Proposition 3.1 (plus  $\nu_{\Sigma_f} \in \mathcal{PW}^{1,\infty}(\mathcal{R})$  for the eigenproblem). We focus again on the  
 448 low-regularity case.

## 449 6.2. A priori error estimates

450 Let  $\mathbf{q} \in \mathbf{H}(\text{div}, \mathcal{R}) \cap \tilde{\mathcal{P}}\mathbf{H}^\mu(\mathcal{R})$ , with  $0 < \mu$ . A global RTN interpolant of  $\mathbf{q}$  is defined on every subdomain  $\tilde{\mathcal{R}}_i$   
 451 via its restriction  $\mathbf{q}_i$ , and denoted by  $\tilde{\mathbf{q}}_{i,R}$  for  $1 \leq i \leq \tilde{N}$ . One may thus define the global interpolant of  $\mathbf{q}$  in  $\tilde{\mathbf{Q}}_h$ ,  
 452 denoted by  $\tilde{\mathbf{q}}_R$  henceforth:  $\tilde{\mathbf{q}}_R|_{\tilde{\mathcal{R}}_i} = \tilde{\mathbf{q}}_{i,R}$  for  $1 \leq i \leq \tilde{N}$ . Below, we also use the orthogonal projection operators  
 453  $\pi^0 : L^2(\mathcal{R}) \rightarrow L_h^0$  (see Sect. 4.5.1) and  $\Pi_S^0 : M \rightarrow M_h^0$  (see Sect. 5.2). One has the following result, whose proof  
 454 is given in Appendix A.

455 **Lemma 6.1.** *Assume that the meshes are nested, non-matching, on the interface  $\Gamma_{fc}$ , and that they are quasi-*  
 456 *uniform on  $\Gamma_{fc}$ . To fix ideas, we assume  $T_{c,h}|\Gamma_{fc} \subset T_{f,h}|\Gamma_{fc}$  with  $T_{c,h}|\Gamma_{fc} \neq T_{f,h}|\Gamma_{fc}$  (<sup>4</sup>).*

457 *Let  $\mathbf{q} \in \mathbf{H}(\text{div}, \mathcal{R}) \cap \mathbf{H}^\mu(\mathcal{R})$  with  $0 < \mu < 1/2$ , it holds:*

$$\|[\tilde{\mathbf{q}}_R \cdot \mathbf{n}]\|_{0,\Gamma_{fc}} \lesssim h_f^{1/2} \|\mathbf{q}_f\|_{\mathbf{H}(\text{div}, \tilde{\mathcal{R}}_f)}.$$

458 **Theorem 6.2.** *Let the assumptions of Proposition 3.1 hold, with  $r_{\max} < 1/2$ . One has for matching meshes:*

$$\begin{aligned} & \forall \mu \in ]0, r_{\max}[, \forall S_f \in H^\mu(\mathcal{R}), \\ & \|\mathbf{p} - \mathbf{p}_h\|_{\mathbf{H}(\text{div}, \mathcal{R})} + \|\phi - \phi_h\|_{0,\mathcal{R}} + \|\phi_S - \phi_{S,h}\|_M \lesssim h^\mu \|S_f\|_{\mu,\mathcal{R}}. \end{aligned} \quad (6.2)$$

459 *For nested, non-matching meshes, the result holds under the assumption that on an interface  $\Gamma_{ij}$  where the*  
 460 *meshes  $T_{i,h}|\Gamma_{ij}$  and  $T_{j,h}|\Gamma_{ij}$  are non-matching ( $T_{i,h}|\Gamma_{ij} \neq T_{j,h}|\Gamma_{ij}$ ), the families of triangulations of  $T_{i,h}|\Gamma_{ij}$  and*  
 461  *$T_{j,h}|\Gamma_{ij}$  are quasi-uniform.*

462 *Proof.* We bound the different contributions in the right-hand side of (6.1) for some appropriately chosen discrete  
 463 field  $\mathbf{w}_h$ . Recall that  $\mathbf{u} = ((\mathbf{p}, \phi), \phi_S)$ .

464 *Matching meshes.* We know that  $[\mathbf{p} \cdot \mathbf{n}] = 0$ . For matching meshes, one has also  $[\tilde{\mathbf{p}}_R \cdot \mathbf{n}] = 0$ , so  $[(\mathbf{p} - \tilde{\mathbf{p}}_R) \cdot \mathbf{n}] = 0$ .  
 465 Starting from (6.1), the conclusion follows. Indeed, according to the *a priori* estimates (4.15), (4.20) and (5.9),  
 466  $\mathbf{w}_h = (\tilde{\mathbf{p}}_R, \pi^0 \phi, \Pi_S^0(\phi_S)) \in \mathbb{W}_h$  is such that

$$\begin{aligned} \|\mathbf{u} - \mathbf{w}_h\|_{\mathbb{W}}^2 &= \sum_{i=1}^{\tilde{N}} \|\mathbf{p}_i - \mathbf{p}_{i,R}\|_{\mathbf{H}(\text{div}, \tilde{\mathcal{R}}_i)}^2 + \|\phi - \pi^0 \phi\|_{0,\mathcal{R}}^2 + \|\phi_S - \Pi_S^0(\phi_S)\|_M^2 \\ &\lesssim h^{2\mu} (\|\mathbf{p}\|_{\mu,\mathcal{R}}^2 + \|\text{div } \mathbf{p}\|_{\mu,\mathcal{R}}^2) + h^2 \|\phi\|_{\mathcal{P}H^1(\mathcal{R})}^2 + h_S \|\phi_S\|_{H^{1/2}(\Gamma_S)}^2 \lesssim h^{2\mu} \|S_f\|_{\mu,\mathcal{R}}^2. \end{aligned}$$

<sup>3</sup>For non-nested meshes, numerical illustrations suggest that the convergence properties can be recovered in some situations (see [13], Tab. 2). See also Section 6.5.

<sup>4</sup>*f* refers to *fine discretization*, while *c* refers to *coarse discretization*.

Hence we conclude that for matching meshes it holds:

$$\|\mathbf{u} - \mathbf{u}_h\|_{\mathbb{W}} \lesssim h^\mu \|S_f\|_{\mu, \mathcal{R}}. \quad (6.3)$$

*Nested meshes.* In this case,  $[\tilde{\mathbf{p}}_R \cdot \mathbf{n}] \neq 0$  in general. Nonetheless, one can use the result of Lemma 6.1, to find that

$$\|[(\mathbf{p} - \tilde{\mathbf{p}}_R) \cdot \mathbf{n}]\|_M \lesssim h^{1/2} \|\mathbf{p}\|_{\mathbf{H}(\text{div}, \mathcal{R})},$$

provided that the meshes are *quasi-uniform* on the part of the interface where they are non-matching. One concludes that the estimate (6.3) still holds for nested meshes under this condition.

*Conclusion.* Noting that it always holds  $[\mathbf{p} \cdot \mathbf{n}] = [\mathbf{p}_h \cdot \mathbf{n}] = 0$  (cf. (5.14)), developing the norm  $\|\mathbf{u} - \mathbf{u}_h\|_{\mathbb{W}}$ , one concludes:

$$\|\mathbf{p} - \mathbf{p}_h\|_{\mathbf{H}(\text{div}, \mathcal{R})} + \|\phi - \phi_h\|_{0, \mathcal{R}} + \|\phi_S - \phi_{S,h}\|_M \lesssim h^\mu \|S_f\|_{\mu, \mathcal{R}}.$$

In other words, we have the *a priori* error estimate (6.2). □

As in the plain case, for “smooth data”  $S_f$ , i.e.  $S_f \in H^{r_{\max}}(\mathcal{R})$ , one expects a convergence rate at least in  $h^{r_{\max}}$ .

**Remark 6.3.** Within our framework, we obtain error estimates that generalize those of [11, 32] for low-regularity solutions. In addition, the technical aspects we propose remain quite simple and natural.

### 6.3. Aubin-Nitsche-type estimates

To derive improved estimates on the error  $\|\phi - \phi_h\|_{0, \mathcal{R}}$ , we adapt the calculations of Section 4.5.2 to the DD case. Recall that  $\mathbf{Q}_h = \tilde{\mathbf{Q}}_h \cap \mathbf{H}(\text{div}, \mathcal{R})$ . We already know that when conditions (5.11)–(5.12) hold, the solution  $((\mathbf{p}_h, \phi_h), \phi_{S,h}) \in \tilde{\mathbf{X}}_h \times M_h$  of (5.10) (discrete DD case) is such that  $(\mathbf{p}_h, \phi_h) \in \mathbf{X}_h$ , since  $\mathbf{p}_h \in \mathbf{Q}_h$ . Then restricting the test-fields in (5.10) to elements of  $\mathbf{X}_h \times M_h$  we observe that  $(\mathbf{p}_h, \phi_h)$  satisfies (4.14) too (discrete plain-case), because all interface terms *vanish*. Hence, to estimate  $\|\phi - \phi_h\|_{0, \mathcal{R}}$  in the DD case, we explicitly consider that the discrete fields  $(\mathbf{p}_h, \phi_h)$  are also the solution to the variational formulation of the plain-case (4.14). Let us begin by a technical result, whose proof is given in Appendix A.

**Lemma 6.4.** *Let the assumptions of Lemma 6.1 hold. Let  $\mathbf{q} \in \mathbf{H}(\text{div}, \mathcal{R}) \cap \mathbf{H}^\mu(\mathcal{R})$  with  $0 < \mu < 1/2$ , and define  $\delta \mathbf{q}_{f_c} \in \mathbf{Q}_{f,h}$  by  $\delta \mathbf{q}_{f_c} \cdot \mathbf{n}|_{\Gamma_{f_c}} = (\tilde{\mathbf{q}}_{c,R} \cdot \mathbf{n} - \tilde{\mathbf{q}}_{f,R} \cdot \mathbf{n})|_{\Gamma_{f_c}}$  and zero extension in  $\tilde{\mathcal{R}}_f \setminus \Gamma_{f_c}$ . It holds*

$$\|\delta \mathbf{q}_{f_c}\|_{\mathbf{H}(\text{div}, \tilde{\mathcal{R}}_f)} \lesssim h^\mu \left( \|\mathbf{q}_f\|_{\mu, \tilde{\mathcal{R}}_f} + \|\text{div } \mathbf{q}_f\|_{0, \tilde{\mathcal{R}}_f} \right).$$

**Theorem 6.5.** *Under the assumptions of Theorem 6.2 with  $r_{\max} < 1/2$ , one has for nested meshes:*

$$\forall \mu \in ]0, r_{\max}[, \forall S_f \in H^\mu(\mathcal{R}), \quad \|\phi - \phi_h\|_{0, \mathcal{R}} \lesssim h^{2\mu} \|S_f\|_{\mu, \mathcal{R}}. \quad (6.4)$$

*Proof. Matching meshes.* In this case, one can use the theory already developed in Section 4.5 for the plain case, to conclude that (6.4) holds.

*Nested meshes.* The difficulty for non-matching meshes is that one cannot define the global RTN-interpolant of  $\mathbf{p}$  directly. Instead it is defined *via* its subdomain interpolants  $(\tilde{\mathbf{p}}_{i,R})_{1 \leq i \leq \tilde{N}}$ . Introduce, for  $1 \leq i \leq \tilde{N}$ ,  $\mathcal{I}_i$  as the set of indices  $j$  such that  $T_{j,h}|\Gamma_{ij} \subset T_{i,h}|\Gamma_{ij}$  (since we are dealing with nested meshes, it holds  $T_{j,h}|\Gamma_{ij} \subset T_{i,h}|\Gamma_{ij}$  or  $T_{i,h}|\Gamma_{ij} \subset T_{j,h}|\Gamma_{ij}$ ). We proceed as follows to obtain an  $\mathbf{H}(\text{div}, \mathcal{R})$ -conforming approximant, i.e. an element of  $\mathbf{Q}_h$ . On all interfaces  $\Gamma_{ij}$ , introduce  $\delta \mathbf{p}_{ij} \cdot \mathbf{n} = \tilde{\mathbf{p}}_{c,R} \cdot \mathbf{n}|_{\Gamma_{ij}} - \tilde{\mathbf{p}}_{f,R} \cdot \mathbf{n}|_{\Gamma_{ij}}$  where  $\tilde{\mathbf{p}}_{f,R}$  is the interpolant from the finer discretization on  $\Gamma_{ij}$ , resp.  $\tilde{\mathbf{p}}_{c,R}$  is the interpolant from the coarser discretization on  $\Gamma_{ij}$ . By construction,

497  $\delta \mathbf{p}_{ij} \cdot \mathbf{n} = 0$  when  $T_{i,h|\Gamma_{ij}} = T_{j,h|\Gamma_{ij}}$ . Then  $\delta \mathbf{p}_{ij} \cdot \mathbf{n}$  is extended by zero in  $\tilde{\mathcal{R}}_i$  to define an element of  $\mathbf{Q}_{i,h}$ ; with a  
 498 slight abuse of notation, we still denote the extension by  $\delta \mathbf{p}_{ij}$ . The  $\mathbf{H}(\text{div}, \mathcal{R})$ -conforming approximant  $\mathbf{p}_R \in \mathbf{Q}_h$   
 499 is then defined subdomain by subdomain as

$$\mathbf{p}_{i,R} = \tilde{\mathbf{p}}_{i,R} + \sum_{j \in \mathcal{I}_i} \delta \mathbf{p}_{ij} \quad \text{for } 1 \leq i \leq \tilde{N}.$$

500 Indeed,  $[\mathbf{p}_R \cdot \mathbf{n}]_{\Gamma_{ij}} = 0$  for  $1 \leq i, j \leq \tilde{N}$  by direct inspection. It remains to evaluate

$$\begin{aligned} \|\mathbf{p} - \mathbf{p}_R\|_{\mathbf{H}(\text{div}, \mathcal{R})}^2 &= \sum_{1 \leq i \leq \tilde{N}} \|\mathbf{p}_i - \mathbf{p}_{i,R}\|_{\mathbf{H}(\text{div}, \tilde{\mathcal{R}}_i)}^2, \quad \text{with} \\ \|\mathbf{p}_i - \mathbf{p}_{i,R}\|_{\mathbf{H}(\text{div}, \tilde{\mathcal{R}}_i)} &\leq \|\mathbf{p}_i - \tilde{\mathbf{p}}_{i,R}\|_{\mathbf{H}(\text{div}, \tilde{\mathcal{R}}_i)} + \sum_{j \in \mathcal{I}_i} \|\delta \mathbf{p}_{ij}\|_{\mathbf{H}(\text{div}, \tilde{\mathcal{R}}_i)} \quad \text{for } 1 \leq i \leq \tilde{N}. \end{aligned}$$

501 Above, the fact that the index  $j$  belongs to  $\mathcal{I}_i$  implies that if  $\delta \mathbf{p}_{ij} \neq 0$ , then the finer discretization on  $\Gamma_{ij}$   
 502 automatically originates from  $\tilde{\mathcal{R}}_i$ . To evaluate  $\|\delta \mathbf{p}_{ij}\|_{\mathbf{H}(\text{div}, \tilde{\mathcal{R}}_i)}$ , one uses the results of Lemma 6.4 to find

$$\|\delta \mathbf{p}_{ij}\|_{\mathbf{H}(\text{div}, \tilde{\mathcal{R}}_i)} \lesssim h^\mu \left( \|\mathbf{p}_i\|_{\mu, \tilde{\mathcal{R}}_i} + \|\text{div } \mathbf{p}_i\|_{0, \tilde{\mathcal{R}}_i} \right).$$

503 Again, this bound holds under the condition that the meshes are *quasi-uniform* on the part of the interface  
 504 where they are non-matching. Due to (4.20), one has  $\|\mathbf{p}_i - \mathbf{p}_{i,R}\|_{\mathbf{H}(\text{div}, \tilde{\mathcal{R}}_i)} \lesssim h^\mu \|S_f\|_{\mu, \mathcal{R}}$  for  $1 \leq i \leq \tilde{N}$ , and it  
 505 follows that

$$\|\mathbf{p} - \mathbf{p}_R\|_{\mathbf{H}(\text{div}, \mathcal{R})} \lesssim h^\mu \|S_f\|_{\mu, \mathcal{R}}.$$

506 As a consequence (follow Sect. 4.5.2) we conclude that the estimate (6.4) holds.  $\square$

## 507 6.4. Numerical analysis of the generalized eigenvalue problem

508 Let us focus on the approximation of the generalized eigenvalue problem (3.2) for low-regularity solutions  
 509 with nested (matching or non-matching) meshes. We will follow the methodology of Section 4.6.

### 510 6.4.1. Convergence in operator norm

511 Let  $0 \leq \mu < r_{\max}$  be given, we introduce an operator  $B_\mu$  associated to the source problem (5.6): given  $f \in$   
 512  $H^\mu(\mathcal{R})$ , we call  $B_\mu f = \phi \in H^1(\mathcal{R})$  the second component of the triple  $(\mathbf{p}, \phi, \phi_S)$  that solves the source problem  
 513 with  $S_f = \underline{\nu} \Sigma_f f$ . For the same reason as in the plain case Section 4.6.1,  $B_\mu$  is a bounded and compact operator.  
 514 Next, let us consider the discrete operator  $B_\mu^h$  associated to the discrete source problem: given  $f \in H^\mu(\mathcal{R})$ , we  
 515 call  $B_\mu^h f$  the second component of the triple  $(\mathbf{p}_h, \phi_h, \phi_{S,h})$  that solves (5.10) with source  $S_f = \underline{\nu} \Sigma_f f$ . Using  
 516 estimate (6.4), we obtain, like in the plain case, the result below.

517 **Theorem 6.6.** *Under the assumptions of Theorem 6.2 with  $r_{\max} < 1/2$  plus  $\underline{\nu} \Sigma_f \in \mathcal{PW}^{1,\infty}(\mathcal{R})$ , let  $\mu \in ]0, r_{\max}[$ .  
 518 Provided that the families of triangulations are regular<sup>+</sup> on every subdomain, one has for nested meshes:*

$$\|B_\mu - B_\mu^h\|_{\mathcal{L}(H^\mu(\mathcal{R}))} \lesssim h^{\tilde{\theta}}, \quad (6.5)$$

519 where  $\tilde{\theta} = \min_{i=1}^{\tilde{N}} \theta_i > 0$ , and for  $1 \leq i \leq \tilde{N}$ ,  $\theta_i$  is defined by (4.29) on  $\tilde{\mathcal{R}}_i$ .

520 We conclude to the absence of spectral pollution.

### 6.4.2. Optimal convergence rate

Let the assumptions of Theorems 6.2 and 6.6 hold, and in particular the conditions for nested, *non-matching* meshes. We use the same notations as in Section 4.6.2. In particular, let  $\tilde{\omega}_\nu > 0$  be the regularity exponent associated to  $\nu$  with respect to  $(\tilde{\mathcal{P}}H^{1+s}(\mathcal{R}))_{s>0}$ , and introduce  $\tilde{\omega} = \min(\tilde{\omega}_\nu, k + 1)$ .

Let  $\mu \in [0, r_{\max}[$  be given. As we defined  $B_\mu$  (resp.  $B_\mu^h$ ), we define  $A_\mu$  and  $C_\mu$  (resp.  $A_\mu^h$  and  $C_\mu^h$ ): for  $f \in H^\mu(\mathcal{R})$ , we call  $A_\mu f = \mathbf{p} \in \tilde{\mathbf{Q}}$  and  $C_\mu f = \phi_S \in M$  (resp.  $A_\mu^h f = \mathbf{p}_h \in \tilde{\mathbf{Q}}_h$  and  $C_\mu^h f = \phi_{S,h} \in M_h$ ) the first and the third components of the triple  $(\mathbf{p}, \phi, \phi_S)$  (resp.  $(\mathbf{p}_h, \phi_h, \phi_{S,h})$ ) that solves (5.6) (resp. (5.10)) with source  $S_f = \underline{\nu} \Sigma_f f$ .

For the DD+ $L^2$ -jumps method, the transposition of Lemma 4.16 reads:

**Lemma 6.7.** *Let  $\varphi$  and  $\varphi'$  be in  $W$ . Then, it holds:*

$$\begin{aligned} (\underline{\nu} \Sigma_f \varphi, (B_\mu - B_\mu^h) \varphi')_{0, \mathcal{R}} &= a(A_\mu \varphi, (A_\mu - A_\mu^h) \varphi') + b((A_\mu - A_\mu^h) \varphi', B_\mu \varphi) \\ &\quad + b(A_\mu \varphi, (B_\mu - B_\mu^h) \varphi') + t(B_\mu \varphi, (B_\mu - B_\mu^h) \varphi'); \end{aligned} \quad (6.6)$$

and

$$\begin{aligned} 0 &= a(A_\mu^h \varphi, (A_\mu - A_\mu^h) \varphi') + b((A_\mu - A_\mu^h) \varphi', B_\mu^h \varphi) \\ &\quad + b(A_\mu^h \varphi, (B_\mu - B_\mu^h) \varphi') + t(B_\mu^h \varphi, (B_\mu - B_\mu^h) \varphi'). \end{aligned} \quad (6.7)$$

The formulas (6.6) and (4.33), resp. (6.7) and (4.34), are identical. As Strang's Lemma holds for the DD+ $L^2$ -jumps method with nested meshes, we can also transpose Proposition 4.17. For that, we admit that the result of Lemma 6.1 can be improved for smooth functions  $\mathbf{q}$ . As a matter of fact, in this case one may directly compare the discrete normal traces  $\Pi_{f,R}(\mathbf{q} \cdot \mathbf{n}_{|\Gamma_{fc}})$  and  $\Pi_{c,R}(\mathbf{q} \cdot \mathbf{n}_{|\Gamma_{fc}})$  to the exact normal trace  $\mathbf{q} \cdot \mathbf{n}_{|\Gamma_{fc}}$ , and evaluate the difference in  $L^2(\Gamma_{fc})$ -norm, because for smooth functions the exact normal trace always belongs to  $L^2(\Gamma_{fc})$ .

**Proposition 6.8.** *For every  $\varphi$  in  $W$ , the following inequalities hold for the DD+ $L^2$ -jumps method with nested meshes:*

$$\begin{aligned} \|(B_\mu - B_\mu^h) \varphi\|_{0, \mathcal{R}} &\lesssim h^{\tilde{\omega}} \|\varphi\|_W; \\ \|(A_\mu - A_\mu^h) \varphi\|_{\mathbf{H}(\text{div}, \mathcal{R})} &\lesssim h^{\tilde{\omega}} \|\varphi\|_W. \end{aligned}$$

Estimate (4.37) on the gap between  $W$  and  $W_h$  is still valid:  $\hat{\delta}(W, W_h) \lesssim h^{\tilde{\omega}}$ . Let  $E_h$  be the operator defined in (4.38). We recall that  $E_h$  and  $B_\mu^h$  commute (Lem. 4.18 holds). The restriction of  $E_h$  to  $W$ , denoted by  $F_h$  is a bijection that satisfies estimate (4.39), for  $h$  small enough. We will also make use of  $\mathcal{S}_h = F_h^{-1} E_h - I$  that satisfies Lemma 4.20 and Proposition 4.21. We recall that  $\hat{B}_\mu = B_\mu|_W$  and  $\hat{B}_\mu^h = F_h^{-1} B_\mu^h F_h$ . The transposition of Theorem 4.22 is stated next. The proof is identical (replace  $\omega$  by  $\tilde{\omega}$ ), so it is omitted.

**Theorem 6.9.** *For  $h$  small enough, one has for the DD+ $L^2$ -jumps method with nested meshes:*

$$\|\hat{B}_\mu - \hat{B}_\mu^h\|_{\mathcal{L}(W)} \lesssim h^{2\tilde{\omega}}. \quad (6.8)$$

**Corollary 6.10.** *For  $h$  small enough, the error on the eigenvalue for the DD+ $L^2$ -jumps method with nested meshes is given by:*

$$|\nu - \nu_h| \lesssim h^{2\tilde{\omega}}.$$



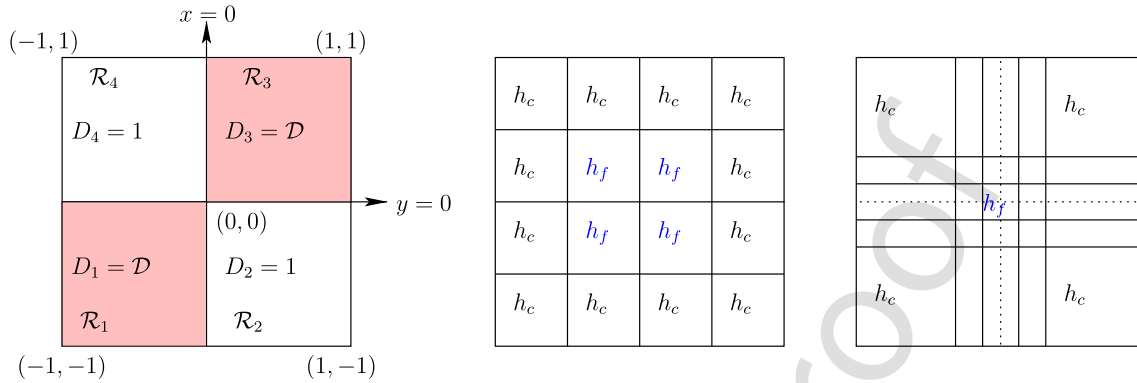


FIGURE 2. The domain of study, and the subdomain mesh sizes.

### 547 6.5. About non-nested meshes

548 We recall that, for general non-nested meshes, one has convergence without explicit convergence rate, as soon  
 549 as (5.11)–(5.12) hold uniformly. In the most general case however, it seems difficult to obtain a convergence  
 550 error that depends explicitly on  $h$ .

551 On the other hand, let us consider the case where the meshes are non-nested, *with some structure*. By  
 552 structure, it is understood that the non-nestedness can be described by a finite number of configurations (*e.g.*  
 553 3-face mesh *vs.* 5-face mesh, etc.) that are reproduced at smaller and smaller scales when the meshsize diminishes.

554 We note first that a result similar to Lemma 6.1 can be recovered. Going back to the reference configurations  
 555 (by assumption there are a finite number of them) and taking the supremum in the upper bounds among all  
 556 these configurations, we infer from (A.5) that  $\|[\tilde{\mathbf{q}}_R \cdot \mathbf{n}]\|_{0, \Gamma_{fc}} \lesssim h_c |_{\Gamma_{fc}} \|q_{f,h}\|_{0, \Gamma_{fc}}$ , *i.e.* one can conclude the  
 557 proof as before. As a consequence, an explicit convergence rate may be derived for the source problem as in  
 558 Theorem 6.2.

559 Then, one may proceed in a similar fashion to prove Lemma 6.4, so as to derive an Aubin-Nitsche estimate  
 560 as in Theorem 6.5. Finally, because interface terms are absent in the analysis of the convergence rate of the  
 561 eigenvalues (see in particular (6.6)–(6.7)), such estimates can also be proved for non-nested meshes, with some  
 562 structure.

## 563 7. NUMERICAL ILLUSTRATIONS

564 The tests are carried out in two dimensions: the cartesian coordinates are denoted by  $(x, y)$ . We use RTN<sub>[0]</sub>  
 565 finite elements on rectangular meshes. We define the discrete space of Lagrange multipliers  $M_h$  as in (5.13).

### 566 7.1. Benchmark square for transmission problems

567 We study a singular toy problem described on Dauge’s website [15] for a magnetic problem and adapted here  
 568 for the neutron diffusion equation with Neuman boundary condition. Set  $\mathcal{R} := ]-1, 1[^2$ , and divide it into four  
 569 subsquares (see Fig. 2 left). Let  $D$ , be a scalar, piecewise-constant, coefficient:  $D := \mathcal{D} = 0.1$  in  $\mathcal{R}_1 \cup \mathcal{R}_3$ , and 1  
 570 elsewhere,  $\Sigma_a = 1$  and  $\nu \Sigma_f = 1$ . We consider the following problem:

$$\begin{cases} -\operatorname{div} D \mathbf{grad} \phi + \phi = \lambda \phi & \text{in } \mathcal{R} \\ \frac{\partial \phi}{\partial n} = 0 & \text{on } \partial \mathcal{R}. \end{cases} \quad (7.1)$$

571 The singularity exponent is  $r_{\max} \approx 0.39$ . Implementation is in MATLAB.

TABLE 1. Results with 16 subdomains.

$1/h$	$N_\phi$	$\varepsilon_{\lambda_1}$	$\varepsilon_{\lambda_2}$	$\varepsilon_{\lambda_3}$	$\varepsilon_{\lambda_4}$
4	448	$2.88 e - 3$	$3.92 e - 2$	$5.49 e - 3$	$2.00 e - 2$
8	1 792	$7.22 e - 4$	$2.36 e - 2$	$1.38 e - 3$	$5.00 e - 3$
12	4 032	$3.22 e - 4$	$1.74 e - 2$	$6.12 e - 4$	$2.22 e - 3$
16	7 168	$1.81 e - 4$	$1.40 e - 2$	$3.44 e - 4$	$1.25 e - 3$
20	11 200	$1.16 e - 4$	$1.18 e - 2$	$2.20 e - 4$	$8.00 e - 4$
24	16 128	$8.05 e - 5$	$1.02 e - 2$	$1.53 e - 4$	$5.05 e - 4$
Rate		$h^2$	$h^{0.76}$	$h^2$	$h^2$

TABLE 2. Results with 25 subdomains using graded meshes.

$1/h$	$N_\phi$	$\varepsilon_{\lambda_1}$	$\varepsilon_{\lambda_2}$	$\varepsilon_{\lambda_3}$	$\varepsilon_{\lambda_4}$
3	304	$7.47 e - 3$	$1.14 e - 2$	$1.92 e - 2$	$1.12 e - 1$
6	1 216	$1.92 e - 3$	$8.19 e - 3$	$4.90 e - 3$	$2.75 e - 2$
12	4 864	$4.83 e - 4$	$5.28 e - 3$	$1.23 e - 3$	$6.85 e - 3$
15	7 600	$3.10 e - 4$	$4.42 e - 3$	$7.88 e - 4$	$4.38 e - 3$
18	10 944	$2.15 e - 4$	$3.86 e - 3$	$5.47 e - 4$	$3.04 e - 3$
21	14 896	$1.59 e - 4$	$6.68 e - 4$	$4.02 e - 4$	$2.24 e - 3$
Rate		$h^2$	$h^{0.71}$	$h^2$	$h^2$

572 We study the error on the four first eigenvalues (excluding  $\lambda_0 = 1$ ), with two different partitions  $\{\tilde{\mathcal{R}}_i\}_{1 \leq i \leq \tilde{N}}$ .  
 573 The results are given in Tables 1 and 2, which data are:

- 574 •  $h$ : the meshsize,
- 575 •  $N_\phi$ : the number of degrees of freedom of  $\phi$ ,
- 576 •  $\varepsilon_{\lambda_i} = |\lambda_{h,i} - \lambda_i|/|\lambda_i|$ : the relative error for the eigenvalue  $\lambda_i$ ,  $i = 1, 4$ .

577 In the last line, we report the average rate of convergence of the computations. In Figure 3a (resp. 3b), we  
 578 represented the mesh for  $1/h = 12$  (resp.  $1/h = 18$ ) and the second non-constant eigenfunction  $\phi_2$ , which is  
 579 singular at the cross-point.

580 The first partition is based on  $\tilde{N} = 16$  square subdomains, represented in Figure 2 middle. As indicated in  
 581 this figure, the four centered subdomains have a meshsize equal to  $h_f$  whereas the other subdomains have a  
 582 meshsize equal to  $h_c = 2h_f$ , so that the parameter is  $h = h_c$ . The results are given in Table 1.

583 The second partition is based on  $\tilde{N} = 25$  subdomains, with graded meshes towards the cross-point, where  
 584 the singular behaviour is expected. The subdomain in the center of  $\mathcal{R}$  has a mesh size equal to  $h_f$ , whereas the  
 585 four subdomains on the corners of  $\mathcal{R}$  have a meshsize equal to  $h_c = 6h_f$  (see Fig. 2 right). This is similar in  
 586 spirit to the XFEM except there is only one mesh near the cross-point [20].

587 The results are given in Table 2. With this simple idea (the use of graded meshes), one derives an accurate  
 588 approximation of the singular eigenfunction at low cost. Indeed, comparing Tables 1 and 2, one notices that the  
 589 error  $\varepsilon_{\lambda_2}$  is comparable using the coarser mesh of the second partition (with  $N_\phi = 304$ ) than using the finer  
 590 mesh of the first partition (with  $N_\phi = 16 128$ ). However, the approximation of eigenvalues associated to smooth  
 591 eigenfunctions is not improved by the use of graded meshes. On the contrary, as the order of the eigenvalues  
 592 increases, their approximations seem to be more and more degraded, which is due to the difficulty to capture  
 593 the faster and faster oscillations of the corresponding eigenfunctions.

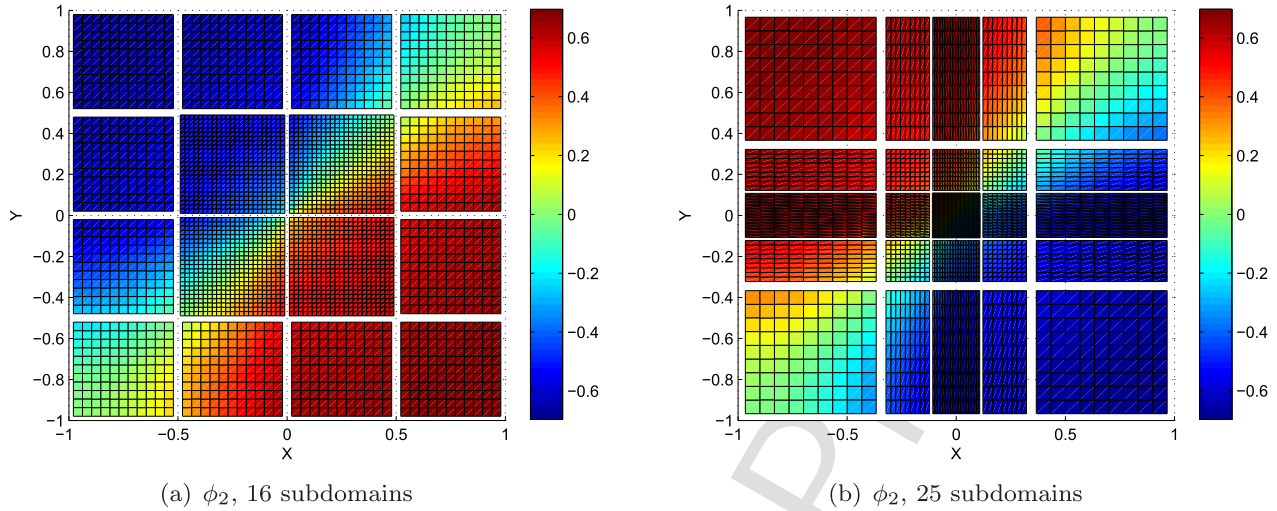


FIGURE 3. The second non-constant eigenfunction.

## 7.2. PWR core

We give here some results of computations carried out with the MINOS solver of the APOLLO3<sup>®5</sup> neutronics code [30] developed at CEA. This industrial test models a pressurized water large reactor core with heavy-steel reflector similar to the one described in [29]. The neutron transport equation is discretized using the multigroup simplified  $P_N$  ( $SP_N$ ) equations, with two groups of energy, and  $SP_1$  and  $SP_3$  angular orders. We recall that, for each group, the neutron  $SP_1$  equation is similar to the neutron diffusion equation, whereas the neutron  $SP_3$  equation corresponds to two coupled neutron diffusion equations. The different homogenization steps that allow to obtain the coefficients of this discretization on square cells lead to 229 different media. The coefficients are thus parametrized according to the medium, the energy group and the angular order, which depend respectively on the position, the energy and the direction of the neutrons. We refer to [23, 24, 25] for more details on the multigroup  $SP_N$  and diffusion neutron equations and the general algorithm to solve them.

The subdomains  $\{\mathcal{R}_i\}_{1 \leq i \leq 361}$  of the partition correspond to the  $19 \times 19$  cells of Figure 1a. In each subdomain, the coarser triangulation is also such that the coefficients are piecewise constant. The meshes of the subdomains are nested.

In neutronics, the quantity of interest is the inverse of the smallest eigenvalue, which is called the criticality, and is denoted by  $k_{eff}$ . Below, we make comparisons on the criticality, the reference value, denoted by  $k_{eff}^{ref}$ , being computed on a conforming mesh made of  $1.5e+7$  (resp.  $7.5e+6$ ) rectangles in  $SP_1$  (resp.  $SP_3$ ).

In Table 3, we present the results obtained with the MINOS solver for different levels of refinement, with  $RTN_{[0]}$  finite elements on rectangles. The data are:

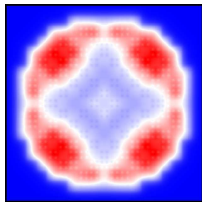
- $h$ : the meshsize,
- $N_\phi$ : the spatial number of degrees of freedom of the neutron flux  $\phi$ ,
- $\varepsilon_1$  (resp.  $\varepsilon_3$ ): the relative error made on the criticality  $|k_{eff} - k_{eff}^{ref}|/k_{eff}^{ref}$ , for a computation using the  $SP_1$  (resp.  $SP_3$ ) approximation.
- rate: the averaged rate of convergence.

Convergence rates are higher than 1, seemingly indicating the absence of strong singularities in the first eigenfunction. Instead, we hypothesize that we are still in the pre-asymptotic regime (for the first eigenfunction):

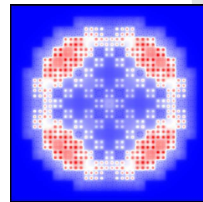
<sup>5</sup>APOLLO3 is a registered trademark in France.

TABLE 3. Results with 361 subdomains.

$1/h$	$N_\phi$	$\varepsilon_1$	$\varepsilon_3$
285	$5.40 e + 5$	$1.35 e - 4$	$1.37 e - 4$
380	$9.60 e + 5$	$8.01 e - 5$	$8.79 e - 5$
570	$2.16 e + 6$	$4.10 e - 5$	$5.12 e - 5$
665	$2.94 e + 6$	$3.26 e - 5$	$4.30 e - 5$
950	$6.00 e + 6$	$2.09 e - 5$	$3.15 e - 5$
Rate		$h^{1.55}$	$h^{1.22}$



(a) First group



(b) Second group

FIGURE 4. Neutron flux.

620 on the one hand, the norm of the “more singular” part is small compared to the norm of the “more regular”  
 621 part, and on the other hand there are only a few degrees of freedom per characteristic length (see Fig. 1b).

622 Note that the DD version is parallelized in the APOLLO3<sup>®</sup> code, contrary to the plain version. Hence,  
 623 computational times are greatly reduced: we refer to [23] for the analyses of algorithms and their parallelization.

624 The neutron flux of the first (resp. second) group of energy are represented in Figure 4a (resp. Fig. 4b).

## 625 8. CONCLUSION

626 The solution of the steady-state one-group neutron diffusion equation being usually of low-regularity, the  
 627 convergence of the eigenvalues and the error estimates are not straightforward to obtain. In particular, we  
 628 provide new proofs:

- 629 • for the source and eigen-problems, with low-regularity solutions;
- 630 • for the eigenproblems, in mixed setting with non-vanishing zero-order term ( $\Sigma_a \neq 0$ ).

631 Notice that our results are obtained under the *regular*<sup>+</sup> condition on the family of triangulations. For the DD  
 632 case, we suggest the following strategies to take into account the apparently restrictive condition on quasi-  
 633 uniform meshes on the interface, compared to the *regular*<sup>+</sup> condition on the family of triangulations:

- 634 • use  $\{\tilde{\mathcal{R}}_i\}_{1 \leq i \leq \tilde{N}}$  for DD as the orthogonal (*i.e.* Voronoï) tessellation of  $\{\mathcal{R}_i\}_{1 \leq i \leq N}$ ;
- 635 • use  $\{\tilde{\mathcal{R}}_i\}_{1 \leq i \leq \tilde{N}} \equiv \{\mathcal{R}_i\}_{1 \leq i \leq N}$  and compute the singular part of the solution (or eigenfunction) *via* some  
 636 *ad hoc* technique (SCM, XFEM, etc.).

637 A possible continuation of this paper is the study of the steady-state multigroup neutron  $SP_N$  problem [21].

## 638 APPENDIX A. ADDITIONAL PROOFS

639 We provide here the proof of three technical lemmas.

640 Let  $(\mathcal{T}_h)_h$  be a given regular family of triangulations. We call  $\hat{K} := [0, 1]^d$  the reference element. Let  $h$  be  
 641 given. For every  $K \in \mathcal{T}_h$ , we denote by  $\mathbf{x} = F_K(\hat{\mathbf{x}}) := \mathbb{A}_K \hat{\mathbf{x}} + \mathbf{b}_K$ ,  $\mathbb{A}_K \in \mathbb{R}^{d \times d}$ ,  $\mathbf{b}_K \in \mathbb{R}^d$ , the map from  $\hat{K}$  to

642  $K$ . Introducing  $h_K = \text{diam}(K)$  for all  $K \in \mathcal{T}_h$ , one may bound  $\|\mathbb{A}_K\|$ ,  $\|(\mathbb{A}_K)^{-1}\|$ ,  $|\det(\mathbb{A}_K)|$  with respect to  $h_K$ .  
 643 The change of variable formulas from  $\hat{K}$  to  $K$ , and vice versa, can be found *e.g.* in Section 1 of [17].

644 *Proof of Lemma 4.13.* We follow Section 2 of [2]. Given  $\psi_h \in L_h^k$ , one has  $\psi_h \in H^\mu(\mathcal{R})$ , for all  $\mu < 1/2$ . By the  
 645 definition of the norm of  $H^\mu(\mathcal{R})$ , we have the following equalities:

$$\begin{aligned} \|\psi_h\|_{\mu, \mathcal{R}}^2 &= \|\psi_h\|_{0, \mathcal{R}}^2 + \int_{\mathcal{R}} \int_{\mathcal{R}} \frac{|\psi_h(\mathbf{x}) - \psi_h(\mathbf{y})|^2}{|\mathbf{x} - \mathbf{y}|^{d+2\mu}} \, d\mathbf{y} d\mathbf{x} \\ &= \sum_{K \in \mathcal{T}_h} \left( \|\psi_h\|_{0, K}^2 + \int_K \int_{\mathcal{R}} \frac{|\psi_h(\mathbf{x}) - \psi_h(\mathbf{y})|^2}{|\mathbf{x} - \mathbf{y}|^{d+2\mu}} \, d\mathbf{y} d\mathbf{x} \right) \\ &= \sum_{K \in \mathcal{T}_h} \|\psi_h\|_{\mu, K}^2 + \sum_{K \in \mathcal{T}_h} \int_K \int_{\mathcal{R} \setminus K} \frac{|\psi_h(\mathbf{x}) - \psi_h(\mathbf{y})|^2}{|\mathbf{x} - \mathbf{y}|^{d+2\mu}} \, d\mathbf{y} d\mathbf{x}. \end{aligned} \quad (\text{A.1})$$

646 Let us estimate first  $\sum_{K \in \mathcal{T}_h} \|\psi_h\|_{\mu, K}^2$ . According to Corollary 1.138 of [17], we know that

$$\sum_{K \in \mathcal{T}_h} \|\psi_h\|_{\mu, K}^2 \lesssim \sum_{K \in \mathcal{T}_h} h_K^{-2\mu} \|\psi_h\|_{0, K}^2 \lesssim h_{\min}^{-2\mu} \|\psi_h\|_{0, \mathcal{R}}^2, \quad (\text{A.2})$$

647 where  $h_{\min} = \min_{K \in \mathcal{T}_h} h_K$ . To estimate the remaining part, we recall that, for any  $K \in \mathcal{T}_h$  and any  $\mathbf{x} \in K$ , it holds  
 648 that, by going back the reference space, applying (*cf.* [22], 1.3.2.12) on  $\hat{K}$  and then going to the physical space:

$$\int_{\mathcal{R} \setminus K} \frac{1}{|\mathbf{x} - \mathbf{y}|^{d+2\mu}} \, d\mathbf{y} \lesssim \frac{1}{\rho_{\partial K}(\mathbf{x})^{2\mu}},$$

649 where  $\rho_{\partial K}(\mathbf{x}) = \inf_{\mathbf{y} \in \partial K} |\mathbf{x} - \mathbf{y}|$ . Thus we have:

$$\begin{aligned} \int_K \int_{\mathcal{R} \setminus K} \frac{|\psi_h(\mathbf{x}) - \psi_h(\mathbf{y})|^2}{|\mathbf{x} - \mathbf{y}|^{d+2\mu}} \, d\mathbf{y} d\mathbf{x} &= \sum_{\substack{K' \in \mathcal{T}_h \\ K' \neq K}} \int_K \int_{K'} \frac{|\psi_h(\mathbf{x}) - \psi_h(\mathbf{y})|^2}{|\mathbf{x} - \mathbf{y}|^{d+2\mu}} \, d\mathbf{y} d\mathbf{x} \\ &\lesssim \sum_{\substack{K' \in \mathcal{T}_h \\ K' \neq K}} \int_K \int_{K'} \frac{\psi_h(\mathbf{x})^2 + \psi_h(\mathbf{y})^2}{|\mathbf{x} - \mathbf{y}|^{d+2\mu}} \, d\mathbf{y} d\mathbf{x} \\ &\lesssim \int_K \frac{\psi_h(\mathbf{x})^2}{\rho_{\partial K}(\mathbf{x})^{2\mu}} \, d\mathbf{x}. \end{aligned} \quad (\text{A.3})$$

650 Going back to the reference element  $\hat{K}$  and introducing  $\psi_{h|K}(\mathbf{x}) = \hat{\psi}(\hat{\mathbf{x}})$ , it stands:

$$\int_K \frac{\psi_h(\mathbf{x})^2}{\rho_{\partial K}(\mathbf{x})^{2\mu}} \, d\mathbf{x} \lesssim h_K^{d-2\mu} \int_{\hat{K}} \frac{\hat{\psi}(\hat{\mathbf{x}})^2}{\rho_{\partial \hat{K}}(\hat{\mathbf{x}})^{2\mu}} \, d\hat{\mathbf{x}}.$$

651 Because  $\mu < 1/2$  (*cf.* [22], Thm. 1.4.4.4),  $\hat{\psi} \mapsto (\int_{\hat{K}} \hat{\psi}(\hat{\mathbf{x}})^2 \rho_{\partial \hat{K}}(\hat{\mathbf{x}})^{-2\mu} \, d\hat{\mathbf{x}})^{1/2}$  is a norm on  $\hat{L}^k = Q_{k,k,k}(\hat{K})$ . Thanks  
 652 to the equivalence of the norms on finite dimensional vector spaces, one gets

$$\int_K \frac{\psi_h(\mathbf{x})^2}{\rho_{\partial K}(\mathbf{x})^{2\mu}} \, d\mathbf{x} \lesssim h_K^{d-2\mu} \|\hat{\psi}\|_{0, \hat{K}}^2.$$

653 Finally, going back to element  $K$ , we know that  $\|\hat{\psi}\|_{0,\hat{K}}^2 \lesssim h_K^{-d} \|\psi_h\|_{0,K}^2$ . Hence using (A.3) and the results that  
 654 follow, we have:

$$\int_K \int_{\mathcal{R} \setminus K} \frac{|\psi_h(\mathbf{x}) - \psi_h(\mathbf{y})|^2}{|\mathbf{x} - \mathbf{y}|^{d+2\mu}} d\mathbf{y} d\mathbf{x} \lesssim h_K^{-2\mu} \|\psi_h\|_{0,K}^2. \quad (\text{A.4})$$

655 Starting from (A.1) using (A.2) and (A.4), we obtain finally the global bound:

$$\|\psi_h\|_{\mu,\mathcal{R}} \lesssim h_{\min}^{-\mu} \|\psi_h\|_{0,\mathcal{R}}.$$

656 As the family of triangulations is *regular*<sup>+</sup>, one has  $h_{\min}^{-\mu} \lesssim h^{(\theta-2)\mu}$ , which concludes the proof.  $\square$

657 *Proof of Lemma 6.1.* For  $l = c, f$ , we introduce the operators from the normal trace spaces  $(\mathbf{H}(\text{div}, \mathcal{R}) \cap$   
 658  $\mathbf{H}^\mu(\mathcal{R})) \cdot \mathbf{n}|_{\Gamma_{fc}}$  to the discrete spaces of normal traces  $T_{l,h}$  on  $\Gamma_{fc}$ :

$$\begin{cases} \Pi_{l,R} : (\mathbf{H}(\text{div}, \mathcal{R}) \cap \mathbf{H}^\mu(\mathcal{R})) \cdot \mathbf{n}|_{\Gamma_{fc}} \rightarrow T_{l,h|\Gamma_{fc}} \\ \mathbf{q}' \cdot \mathbf{n}|_{\Gamma_{fc}} \mapsto \tilde{\mathbf{q}}'_{l,R} \cdot \mathbf{n}|_{\Gamma_{fc}} \end{cases}$$

659 With a slight abuse of notations, we write  $\Pi_{l,R}(\mathbf{q}'_l \cdot \mathbf{n}|_{\partial\tilde{\mathcal{R}}_l}) = \tilde{\mathbf{q}}'_{l,R} \cdot \mathbf{n}|_{\partial\tilde{\mathcal{R}}_l}$ . We also introduce the operator  $\Pi_{c,R}^0$   
 660 on the vector space of normal traces of elements of  $\mathbf{Q}_{c,h}$  with lowest-order RTN finite element, *i.e.* the vector  
 661 space  $T_{c,h|\Gamma_{fc}}^0$  of piecewise constant functions on the interface mesh defined as the trace on  $\Gamma_{fc}$  of the mesh used  
 662 in  $\tilde{\mathcal{R}}_c$ . Note that because the meshes are nested, the restriction of  $\Pi_{f,R}$  (resp.,  $\Pi_{c,R}$  and  $\Pi_{c,R}^0$ ) on  $T_{f,h|\Gamma_{fc}}$  (resp.,  
 663 on the subspaces  $T_{c,h|\Gamma_{fc}}$  and  $T_{c,h|\Gamma_{fc}}^0$  where applicable) may also be considered as an orthogonal projection  
 664 operator. Denoting  $q_{f,h} = \Pi_{f,R}(\mathbf{q} \cdot \mathbf{n}|_{\Gamma_{fc}})$ , we have:

$$\begin{aligned} \|\tilde{\mathbf{q}}_R \cdot \mathbf{n}\|_{0,\Gamma_{fc}} &= \|\Pi_{f,R}(\mathbf{q} \cdot \mathbf{n}|_{\Gamma_{fc}}) - \Pi_{c,R}(\mathbf{q} \cdot \mathbf{n}|_{\Gamma_{fc}})\|_{0,\Gamma_{fc}} \\ &= \|\Pi_{f,R}(\mathbf{q} \cdot \mathbf{n}|_{\Gamma_{fc}}) - \Pi_{c,R} \circ \Pi_{f,R}(\mathbf{q} \cdot \mathbf{n}|_{\Gamma_{fc}})\|_{0,\Gamma_{fc}} \\ &= \|(\mathbb{I} - \Pi_{c,R})q_{f,h}\|_{0,\Gamma_{fc}} \\ &\leq \|(\mathbb{I} - \Pi_{c,R}^0)q_{f,h}\|_{0,\Gamma_{fc}}. \end{aligned} \quad (\text{A.5})$$

665 As the meshes are quasi-uniform on the interface, one has  $h_{c|\Gamma_{fc}} \approx h_{f|\Gamma_{fc}}$ . Then, starting from (A.5), thanks to  
 666 the quasi-uniform mesh assumption for the inverse inequalities on  $\Gamma_{fc}$ , *cf.* Lemma 10.10 of [31], we find

$$\begin{aligned} \|\tilde{\mathbf{q}}_R \cdot \mathbf{n}\|_{0,\Gamma_{fc}} &\lesssim h_{c|\Gamma_{fc}} \|q_{f,h}\|_{0,\Gamma_{fc}} \quad ([3], \text{Lem. 4.9}) \\ &\lesssim h_{c|\Gamma_{fc}} (h_{f|\Gamma_{fc}})^{-1/4} \|q_{f,h}\|_{-1/4,\Gamma_{fc}} \\ &\lesssim (h_{f|\Gamma_{fc}})^{3/4} \|\Pi_{f,R}(\mathbf{q} \cdot \mathbf{n}|_{\partial\tilde{\mathcal{R}}_f})\|_{-1/4,\partial\tilde{\mathcal{R}}_f} \\ &\lesssim (h_{f|\Gamma_{fc}})^{3/4} (h_{f|\partial\tilde{\mathcal{R}}_f})^{-1/4} \|\tilde{\mathbf{q}}_{f,R} \cdot \mathbf{n}|_{\partial\tilde{\mathcal{R}}_f}\|_{-1/2,\partial\tilde{\mathcal{R}}_f} \\ &\lesssim h_f^{1/2} \|\tilde{\mathbf{q}}_{f,R}\|_{\mathbf{H}(\text{div}, \tilde{\mathcal{R}}_f)} \lesssim h_f^{1/2} \|\mathbf{q}_f\|_{\mathbf{H}(\text{div}, \tilde{\mathcal{R}}_f)}. \end{aligned}$$

667 Above, we have used the continuity of the normal trace, resp. the stability of the RTN interpolant, to derive  
 668 the last two inequalities.  $\square$

669 *Proof of Lemma 6.4.* First, let us bound the norm of  $\|\delta\mathbf{q}_{fc}\|_{\mathbf{H}(\text{div}, \tilde{\mathcal{R}}_f)}$  by  $\|\delta\mathbf{q}_{fc} \cdot \mathbf{n}\|_{0,\Gamma_{fc}}$ . We use the notation  
 670  $\mathbf{v} = \delta\mathbf{q}_{fc}$  below. Denoting by  $(K_\ell)_\ell$  the parallelepipeds composing the mesh on  $\tilde{\mathcal{R}}_f$ , and  $\mathcal{N}_\Gamma$  the set of indices  $\ell$

671 such that  $\Gamma_\ell := K_\ell \cap \Gamma_{fc}$  is of Hausdorff dimension  $d - 1$ , because of the definition of  $\mathbf{v}$  it now holds

$$\|\mathbf{v}\|_{\mathbf{H}(\text{div}, \tilde{\mathcal{R}}_f)}^2 = \sum_{\ell} \|\mathbf{v}|_{K_\ell}\|_{\mathbf{H}(\text{div}, K_\ell)}^2 = \sum_{\ell \in \mathcal{N}_\Gamma} \|\mathbf{v}|_{K_\ell}\|_{\mathbf{H}(\text{div}, K_\ell)}^2.$$

672 Then, one can bound  $\|\mathbf{v}|_{K_\ell}\|_{\mathbf{H}(\text{div}, K_\ell)}$  by  $\|\mathbf{v}|_{K_\ell} \cdot \mathbf{n}\|_{0, \Gamma_\ell}$  for each index  $\ell \in \mathcal{N}_\Gamma$ . To that aim, one goes back to  
673 the reference element  $\hat{K}$  via the Piola transform, which reads ([7], Sect. 2.1.3):

$$\mathbf{v}|_{K_\ell}(\mathbf{x}) = \frac{1}{|\det(\mathbb{A}_{K_\ell})|} \mathbb{A}_{K_\ell} \hat{\mathbf{v}}(\hat{\mathbf{x}}), \quad \text{div } \mathbf{v}|_{K_\ell}(\mathbf{x}) = \frac{1}{|\det(\mathbb{A}_{K_\ell})|} \hat{\text{div}} \hat{\mathbf{v}}(\hat{\mathbf{x}}).$$

674 With the help of a classical formula for the change of variables on  $\Gamma_\ell$  ([7], Eq. (2.1.62)), one finds after a few  
675 elementary algebraic manipulations<sup>6</sup> that

$$h_{K_\ell}^{d-1} \int_{\Gamma_\ell} (\mathbf{v}|_{K_\ell} \cdot \mathbf{n})^2 d\Gamma \approx \int_{\hat{\Gamma}_\ell} (\hat{\mathbf{v}} \cdot \hat{\mathbf{n}})^2 d\hat{\Gamma},$$

676 where  $\hat{\Gamma}_\ell$  is equal to  $F_{K_\ell}^{-1}(\Gamma_\ell)$ .

677 On the reference element, it holds

$$\|\hat{\mathbf{v}}\|_{\mathbf{H}(\hat{\text{div}}, \hat{K})}^2 \lesssim \int_{\hat{\Gamma}_\ell} (\hat{\mathbf{v}} \cdot \hat{\mathbf{n}})^2 d\hat{\Gamma},$$

678 because the non-zero degrees of freedom are all located on  $\hat{\Gamma}_\ell$ . Finally, one has the classical bounds ([7], Lem.  
679 2.1.7):

$$\|\mathbf{v}|_{K_\ell}\|_{0, K_\ell}^2 \lesssim h_{K_\ell}^{2-d} \|\hat{\mathbf{v}}\|_{0, \hat{K}}^2, \quad \|\text{div } \mathbf{v}|_{K_\ell}\|_{0, K_\ell}^2 \lesssim h_{K_\ell}^{-d} \|\hat{\text{div}} \hat{\mathbf{v}}\|_{0, \hat{K}}^2,$$

680 so that

$$\|\mathbf{v}|_{K_\ell}\|_{\mathbf{H}(\text{div}, K_\ell)}^2 \lesssim h_{K_\ell}^{-d} \|\hat{\mathbf{v}}\|_{\mathbf{H}(\hat{\text{div}}, \hat{K})}^2 \lesssim h_{K_\ell}^{-1} \int_{\Gamma_\ell} (\mathbf{v}|_{K_\ell} \cdot \mathbf{n})^2 d\Gamma.$$

681 Adding up the contributions for  $\ell \in \mathcal{N}_\Gamma$ , one finds:

$$\|\delta \mathbf{q}_{fc}\|_{\mathbf{H}(\text{div}, \tilde{\mathcal{R}}_f)} \lesssim h_f^{-1/2} \|\delta \mathbf{q}_{fc} \cdot \mathbf{n}\|_{0, \Gamma_{fc}}. \quad (\text{A.6})$$

682 By modifying the final computations in the proof of Lemma 6.1, one finds that for all  $0 < \epsilon < \mu$ :

$$\begin{aligned} \|\delta \mathbf{q}_{fc} \cdot \mathbf{n}\|_{0, \Gamma_{fc}} &\lesssim h_{c|\Gamma_{fc}} \|q_{f,h}\|_{0, \Gamma_{fc}} \quad ([3], \text{Lem. 4.9}) \\ &\lesssim h_{c|\Gamma_{fc}} (h_{f|\Gamma_{fc}})^{\epsilon-1/2} \|q_{f,h}\|_{\epsilon-1/2, \Gamma_{fc}} \quad ([31], \text{Lem. 10.10}) \\ &\lesssim h_f^{\epsilon+1/2} \|q_{f,h}\|_{\epsilon-1/2, \Gamma_{fc}} \\ &\lesssim h_f^{\epsilon+1/2} \|\Pi_{f,R}(\mathbf{q}_f \cdot \mathbf{n}|_{\partial \tilde{\mathcal{R}}_f})\|_{\epsilon-1/2, \partial \tilde{\mathcal{R}}_f} \\ &\lesssim h_f^{\epsilon+1/2} \|\mathbf{q}_f \cdot \mathbf{n}|_{\partial \tilde{\mathcal{R}}_f}\|_{\epsilon-1/2, \partial \tilde{\mathcal{R}}_f} \quad ([2], \text{Thm. 2.4 and Rem. 2.5}) \\ &\lesssim h_f^{\epsilon+1/2} \left( \|\mathbf{q}_f\|_{\epsilon, \tilde{\mathcal{R}}_f} + \|\text{div } \mathbf{q}_f\|_{0, \tilde{\mathcal{R}}_f} \right). \end{aligned}$$

<sup>6</sup>Since the meshes are quasi-uniform on  $\Gamma_{fc}$ , they are in particular regular.

Or, choosing  $\epsilon = \mu - \eta$  for  $\eta > 0$  arbitrary small, that

$$\|\delta \mathbf{q}_{fc} \cdot \mathbf{n}\|_{0, \Gamma_{fc}} \lesssim h_f^{\mu+1/2-\eta} \left( \|\mathbf{q}_f\|_{\mu, \tilde{\mathcal{R}}_f} + \|\operatorname{div} \mathbf{q}_f\|_{0, \tilde{\mathcal{R}}_f} \right).$$

Using (A.6), we conclude the proof.  $\square$

*Acknowledgements.* L. Giret and E. Jamelot gratefully acknowledge EDF for its long term partnership and its support.

## REFERENCES

- [1] I. Babuska and J. Osborn, Eigenvalue problems, in Handbook of Numerical Analysis, edited by P.G. Ciarlet and J.-L. Lions. North Holland (1991) Vol. II, 641–787.
- [2] F. Ben Belgacem and S. Brenner, Some nonstandard finite element estimates with applications to 3D Poisson and Signorini problems. *Electron. Trans. Numer. Anal.* **12** (2001) 134–148.
- [3] A. Bermudez, P. Gamallo, M.R. Nogueiras and R. Rodriguez, Approximation of a structural acoustic vibration problem by hexahedral finite elements. *IMA J. Numer. Anal.* **26** (2006) 391–421.
- [4] D. Boffi, Finite element approximation of eigenvalue problems. *Acta Numer.* **19** (2010) 1–120.
- [5] D. Boffi, F. Brezzi and L. Gastaldi, On the convergence of eigenvalues for mixed formulations. *Ann. Scuola Norm. Sup. Pisa Cl. Sci. Ser. 4* **25** (1997) 131–154.
- [6] D. Boffi, F. Brezzi and L. Gastaldi, On the problem of spurious eigenvalues in the approximation of linear elliptic problems in mixed form. *Math. Comput.* **69** (2000) 121–140.
- [7] D. Boffi, F. Brezzi and M. Fortin, Mixed and Hybrid Finite Element Methods and Applications. Springer-Verlag (2013).
- [8] D. Boffi, D. Gallistl, F. Gardini and L. Gastaldi, Optimal convergence of adaptive FEM for eigenvalue clusters in mixed form. *Math. Comput.* **86** (2017) 2213–2237.
- [9] A. Bonito, J.-L. Guermond and F. Luddens, Regularity of the Maxwell equations in heterogeneous media and Lipschitz domains. *J. Math. Anal. Appl.* **408** (2013) 498–512.
- [10] D. Braess and R. Verfürth, A posteriori error estimators for the Raviart-Thomas element. *SIAM J. Numer. Anal.* **33** (1996) 2431–2444.
- [11] S.C. Brenner, A multigrid algorithm for the lowest-order Raviart-Thomas mixed triangular finite element method. *SIAM J. Numer. Anal.* **29** (1992) 647–678.
- [12] J. Bussac and P. Reuss, *Traité de neutronique*. Hermann (1985).
- [13] P. Ciarlet Jr. E. Jamelot and F.D. Kpadonou, Domain decomposition methods for the diffusion equation with low-regularity solution. *Comput. Math. Appl.* **74** (2017) 2369–2384.
- [14] M. Costabel, M. Dauge and S. Nicaise, Singularities of maxwell interface problems. *ESAIM: M2AN* **33** (1999) 627–649.
- [15] M. Dauge, Benchmark Computations for Maxwell Equations. Available at: <https://perso.univ-rennes1.fr/monique.dauge/core/index.html> (2018).
- [16] J.J. Duderstadt and L.J. Hamilton, Nuclear Reactor Analysis. John Wiley & Sons, Inc. (1976).
- [17] A. Ern and J.-L. Guermond, Theory and Practice of Finite Elements. Springer-Verlag (2004).
- [18] R.S. Falk and J.E. Osborn, Error estimates for mixed methods. *RAIRO Anal. Numer.* **14** (1980) 249–277.
- [19] P. Fernandes and G. Gilardi, Magnetostatic and electrostatic problems in inhomogeneous anisotropic media with irregular boundary and mixed boundary conditions. *Math. Models Methods Appl. Sci.* **7** (1997) 957–991.
- [20] T.-P. Fries and T. Belytschko, The extended/generalized finite element method: an overview of the method and its applications. *Int. J. Numer. Methods Eng.* **84** (2010) 253–304.
- [21] L. Giret, *Non-conforming Domain Decomposition for the Multigroup Neutron  $SP_N$  Equations*. Ph.D. thesis, EDMH, Université Paris-Saclay (2018).
- [22] P. Grisvard, Elliptic Problems in Nonsmooth Domains. Pitman (1985).
- [23] E. Jamelot and P. Ciarlet Jr. Fast non-overlapping Schwarz domain decomposition methods for solving the neutron diffusion equation. *J. Comput. Phys.* **241** (2013) 445–463.
- [24] E. Jamelot, A.-M. Baudron and J.-J. Lautard, Domain decomposition for the  $SP_N$  solver MINOS. *Transp. Theory Stat. Phys.* **41** (2012) 495–512.
- [25] E. Jamelot Jr. P. Ciarlet, A.-M. Baudron and J.-J. Lautard, Domain decomposition for the neutron  $SP_N$  equations, in 21st International Domain Decomposition Conference. Vol. 98 of *Lecture Notes in Computational Science and Engineering* (2014) 677–685.
- [26] J.-C. Nédélec, Mixed finite elements in  $\mathbb{R}^3$ . *Numer. Math.* **35** (1980) 315–341.
- [27] J.E. Osborn, Spectral approximation for compact operators. *Math. Comput.* **29** (1975) 712–725.
- [28] P.-A. Raviart and J.-M. Thomas, A mixed finite element method for second order elliptic problems, in Mathematical Aspects of Finite Element Methods. Vol. 606 of *Lecture Notes in Mathematics*. Springer (1977) 292–315.
- [29] A. Sargeni, K.W. Burn and G.B. Bruna, Coupling effects in large reactor cores: the impact of heavy and conventional reflectors on power distribution perturbations, in *PHYSOR 2014, Kyoto, Japan, Sept 28–Oct 3, 2014* (2014).



- 736 [30] D. Schneider, F. Dolci, F. Gabriel, J.-M. Palau, M. Guillo, B. Pothet *et al.*, APOLLO3®: CEA/DEN deterministic multi-  
737 purpose code for reactor physics analysis, in *PHYSOR 2016, Sun Valley ID, USA, May 1–5, 2016* (2016).
- 738 [31] O. Steinbach, *Numerical Approximation Methods for Elliptic Boundary Value Problems*. Springer, New York (2008).
- 739 [32] M.F. Wheeler and I. Yotov, A posteriori error estimates for the mortar mixed finite element method. *SIAM J. Numer. Anal.*  
740 **43** (2005) 1021–1042.

Uncorrected Proof